Master's Thesis

Studying the Physical State of Phages Using Dynamic Light Scattering (DLS)

Hanieh Shirvani

University of Jyväskylä

Department of Biological and Environmental Science

Nanoscience

20.08.2024

UNIVERSITY OF JYVÄSKYLÄ Abstract of Master's Thesis
Faculty of Mathematics and Science

Author**:**	Hanieh Shirvani
Title of thesis**:**	Studying the Physical State of Phages Using Dynamic Light Scattering (DLS)
Date:	28.07.2024 **Pages:** 61 p., 2 appendices
Department:	Department of Biological and Environmental Science
Chair:	Nanoscience
Supervisors:	Lotta-Riina Sundberg (Professor in Cell and Molecular Biology), Elina Laanto (Assistant Professor), Kaisa Helttunen (Assistant Professor)

Abstract

Bacteriophages are viruses that infect bacteria and have the potential to serve as an alternative to antibiotic treatments for illnesses caused by multidrug-resistant bacteria. However, there remains a critical need to develop improved tools for monitoring their stability and bioactivity. Dynamic light scattering (DLS) may offer several advantages over plaque assay for determining phage stability, such as being quicker, more effective, and less damaging. This method measures the Brownian motion of phages in solution caused by bombardment from solvent molecules and links this motion to particle size. Our goal was to investigate whether DLS can be used in phage research and to examine the effect of different treatments on phages physical state. For this purpose, we examined two phages, T4 and PRD1, with their respective host strains of *E. coli* DMS616 and *Salmonella enterica* DS88. We used DLS to monitor the sizes of phage particles and investigate the changes triggered by sonication and heating. Both methods led to aggregation and an increase in the z-average. Furthermore, the sonication method caused the denaturation of phages and the formation of multiple sharp peaks. Our studies showed that DLS can be used to investigate the physical state of phages. By examining the correlation coefficient versus time plot, it was observed that the purified samples of intact phage particles had an intercept close to 1. Samples with intercepts significantly higher or lower than 1 indicated an underlying issue with the data, such as aggregation. Multiple shoulders indicated a heterogeneous sample. The intensity-weighted distribution provided the most accurate particle size measurements for monodisperse samples. However, for polydisperse samples, the volume distribution offered a better representation of the contribution of different particle sizes to the overall sample volume.

Keywords: dynamic light scattering, phage, therapy, T4, PRD1, antibiotic resistance

Table of Contents

ABBREVIATIONS

AFM	Atomic Force Microscopy
BSA	Bovine serum albumin
Cryo-EM	cryogenic electron microscopy
DLS	Dynamic light scattering
PBS	Phosphate-buffered saline
PCS	photon correlation spectroscopy
PEG	Polyethylene glycol
PDI	Polydispersity index
PFUs	Plaque-forming units
SEM	Scanning electron microscope
MADLS	Multi-Angle Dynamic Light Scattering

1. INTRODUCTION

1.1. Introduction to phages

Bacteriophages, or phages for short, are viruses that specifically infect bacteria and are approximately 50 times smaller than bacteria (20–200 nm) (Ranveer et al. 2024). The term "bacteriophage" originates from the Greek words "bacterio" (meaning bacteria) and "phage" (meaning eat or devour) (Goodridge and Abedon 2002). Phages exhibit a wide range of diversity in their morphology, genetics, and life cycles. Most phages infect only a small subset of host strains (Drulis-Kawa et al. 2015).

Phages attach to the host cell's surface and bind to a specific phage receptor before injecting their genome into the bacterial cell. Depending on the infection type, the following steps may vary: They do not always kill bacteria, and they can have a variety of interactions with their bacterial hosts. Lysogenic or temperate and lytic, or virulent, are the two categories of infection under which phages can be classified (Inal 2003). The lytic cycle degrades host DNA and produces various proteins such as capsid protein, lysis protein, and so on. From these, new phage particles are assembled within the bacterial cell. Phages employ the host's synthetic machinery to manufacture roughly 50–200 phages, which pressure the bacterial cell wall, causing the cell to rupture and release the phages (Goodridge and Abedon 2002). In the lysogenic life cycle, phage DNA gets integrated into host DNA and replicated along with host DNA, thereby remaining cryptic entities. The incorporated phage DNA is referred to as prophage. Lytic genes are present in temperate bacteriophages but are not expressed (Jiang and Paul 1998). Ultimately, the virulent genes are expressed during their life cycle, and the lysogenic life cycle turns into a lytic cycle.

1.2. Bacteriophages against antibiotic-resistant bacteria

Phages are naturally adapted to target bacterial infections due to their abundance in nature and long history of coexistence with bacteria. Phages are being considered as a possible treatment for bacterial infections because of the fast worldwide spread of bacteria that are resistant to multiple drugs and the decrease in the development of new antibiotics. Being naturally occurring, highly specific, and capable of evolution are just a few of the many benefits that phages offer as prospective antibacterial agents (Zalewska-Piątek 2023). Thanks to their extreme specificity, phages can wipe out dangerous bacteria while sparing beneficial bacteria and human cells from harm (Rahimi-Midani et al. 2021). Bacteriophages can evolve quickly to overcome bacterial resistance, aiding in the prevention of resistance development (Eaves E. 2018). Additionally, phages can treat a wide variety of bacterial infections due to their extreme diversity. Therefore, they have the potential to treat bacterial infections, either alone or in combination with antibiotics.

However, a deeper understanding of their structure, function, and stability is essential to optimize their effectiveness in combating infections.

1.3. History of Phage Research

In 1915, a paper was published by Twort, a British bacteriologist, which detailed the discovery of an agent with the ability to cause bacterial lysis. However at that moment, he failed to identify the agent as a virus, and he was beginning to suspect an enzyme. There was initially a lack of interest in his work. Around the same time, Félix d'Hérelle (d'Hérelle 1917), a French-Canadian microbiologist at the Pasteur Institute in Paris, discovered bacteriophages independently. In 1917, d'Hérelle published his research, correctly identifying the bacteriophage as a virus that infects and kills bacteria. He coined the term "bacteriophage" to describe these entities.

In the 1920s and 1930s, scientists from all over the globe studied phages to see if they could treat human infections caused by bacteria. In the 1940s, the pharmaceutical corporation Eli Lilly produced phages in the United States for human use, promoting them to treat various bacterial infections, including wounds and upper respiratory tract infections (Sulakvelidze et al. 2001). The phages did not appear to work well, perhaps due to poor storage or purification; moreover, it was unknown back then that many phages were quite selective about the bacteria they infected. When antibiotics were introduced in the mid-20th century, phage treatment became less popular in the US and most of Europe ("Seeking the Path of Least Resistance" 2019). There was a revival of interest in phage therapy in the late 20th and early 21st centuries, driven by concerns about antibiotic resistance and its limitations. However, there are still obstacles to implementing phage treatment in Europe, even though many reported successful cases of patients treated with phages have been reported. Several clinical trials are taking place in the US and Europe to make phage treatment widely available (Royer et al. 2021).

1.4. Conventional Phage Detection Methods

When it comes to phage therapy, phage counting techniques are crucial to help with dosage determination, quality control, and monitoring phage dynamics. All phases of phage therapy, from development to production to implementation and monitoring, rely on phage counting methods. Increasing our understanding of phage biology and therapeutic processes, improving treatment outcomes, and ensuring product standards and safety all depend on precise phage activity testing (Daubie et al. 2022).

1.4.1. Double agar overlay plaque assay

The double agar overlay plaque test is the gold standard for phage enumeration. This is a quantitative technique on a solid medium in which a densely growing bacterial culture is exposed to several phage dilutions, using one Petri dish per phage dilution. Creating and testing serial dilutions aims to produce a "countable"

number of plaques on a plate. Phage dilutions are mixed with the bacterial strain in a soft agar matrix uniformly distributed over a solid agar medium and incubated, typically overnight. Individual infected cells produce phages, which infect neighboring cells in the bacterial layer. Multiple rounds of infection occur until bacterial growth on the plate stops due to nutritional depletion. This will form discrete holes, or plaques, a zone lacking bacterial growth induced by the proliferation of a single phage particle. Plaques will merge into larger areas devoid of cells if the number of infectious particles is too high (Daubie et al. 2022).

Theoretically and under most circumstances, each plaque began from a single phage infecting a single bacterial cell. Therefore, counting the plaques allows us to determine the number of plaque-forming units (PFUs) in the starting suspension (Abedon 2018).

Plaque morphology, which can be unique to each phage, reveals details about its biology—such as lytic activity and genetic characteristics—with variations in plaque size reflecting differences in lytic activity, replication efficiency, and diffusion rate within the agar medium (Abedon 2018). Some phages produce large, clear plaques, while others create smaller, turbid plaques. Plaques can come in various shapes, including round, irregular, and transparent, with fuzzy edges. The growth pattern of the host bacteria and the distribution of phages within the agar may influence plaque shape. Plaques can be transparent or opaque, depending on the bacterial lysis level and phage progeny release. Highly virulent or lytic strains produce clear plaques due to complete cell death, whereas strains that only kill some of their hosts or that only slow cell growth produce turbid plaques (Ramesh et al. 2019).

Double agar overlay plaque assay is a reliable method to measure the number of infective phages, but it has several limitations. Plaque assay is only applicable to phages that form countable plaques (Toister et al. 2024). Therefore, the selection of an appropriate host strain that the phage can infect is crucial for accurately determining phage concentration (Han and Yang 2014).

Plaque assays can be time-consuming, especially when dealing with slow-growing bacteria or phages with long latent periods. Plaques can take hours or even days to become visible, delaying the results (Han and Yang 2014). For instance, Plaque assays with mycobacteriophages can take 3-5 days due to the slow growth of *Mycobacterium smegmatis* and the phages' long latent periods (Karuppannan et al., 2024).

Plaques must be counted accurately, which requires skill and attention to detail. High plaque counts are challenging because of plaque overlap on plates, which can lead to plaque undercounting (Abedon and Katsaounis 2019). Plaque size and morphology can vary depending on growth conditions, phage infection efficiency, and host bacterial characteristics. Variability in plaque size and morphology can make phage concentration difficult to accurately quantify.

Some phages may be sensitive to antibiotics or chemicals found in the growth medium, which inhibits plaque formation. For example, studies have shown that anionic synthetic polymers can inhibit bacteriophage infection (Marton et al. 2023) and aminoglycoside antibiotics can inhibit phage infection by blocking an early

stage of the infection cycle ("Aminoglycoside Antibiotics Inhibit Phage Infection" n.d.). This can have an impact on the assay's accuracy, especially if the sample contains antibiotic residues or other inhibitory substances. The plaque assay's sensitivity depends on its ability to detect individual plaques. If the phage concentration in the sample is extremely low, it may be difficult to distinguish individual plaques from background noise, resulting in inaccurate quantification.

1.4.2. Advanced microscopic techniques

Phages are often smaller than the wavelengths of light used in light microscopy, making them invisible with this approach. However, scanning electron microscopy (SEM), Atomic force microscopy (AFM) and cryogenic electron microscopy (cryo-EM) have been proven to be a valuable tool in phage research, providing detailed structural and functional insights into these biological entities. For example, Obořilová et al. (2021) used AFM in liquid to monitor the lytic activity of phages on *Staphylococcus aureus*, offering insights into changes in cellular stiffness during the lysis process. Leroux et al. (2018) used SEM to ascertain the binding of phage to clinically relevant *A. Baumannii* isolates. In a study by Li et al. (2023) the structure of bacteriophage E217 before and after DNA ejection was determined using cryo-EM. In this study, a high-titer phage stock of approximately 10^{10} PFU/mL was used to ensure clear visualization of the phage particles.

1.5. DLS as a Potential Method for Phage Enumeration

1.5.1. Insight into DLS Theory: Understanding the Principles

Dynamic Light Scattering (DLS), also known as photon correlation spectroscopy (PCS), is a popular method for determining the homogeneity, size, size distribution and shape of particles in suspension (Thomas et al. 2017). The Brownian motion theory, established by Albert Einstein in 1905, is the foundation of DLS (Haar 1969). Brownian motion is based on the idea that particles constantly collide with solvent molecules; the energy transferred during these collisions causes the particles to move randomly in all directions. The mobility of particles is affected by the size, temperature, and viscosity of the solvent. As a result, knowing the exact temperature is critical for DLS measurements, because the viscosity of the solvent varies with temperature (Harding and Jumel 1998).

When a monochromatic beam of light hits particles, part of the incident light can be transferred or absorbed by the sample. Additionally, if the particles are small enough compared to the wavelength of the radiation, the light scatters in all directions (Rayleigh scattering). The scattering pattern is influenced by the size and shape of the particles, and the intensity of the scattered light is measured by a detector (Stetefeld et al. 2016).

Small particles move faster, and the intensity of light changes more rapidly. Conversely, larger particles move slower, and the scattered light changes more

slowly. If all the other factors influencing particle movement are known, the hydrodynamic diameter can be measured by the particle speed. The digital autocorrelator correlates the scattered light intensity variations with respect to time to estimate the rate of fluctuation, which is related to the diffusion behavior of macromolecules. The Stokes-Einstein (equation 1) relates the diffusion coefficient and the particle diameter (Stetefeld et al. 2016).

$$d(H) = k_B T / 6\pi\eta R_h \quad (1)$$

R_h: hydrodynamic diameter of an equivalent spherical particle (nm); k_B: Boltzmann constant (1.38×10^{-23} J·K^{-1}); T: absolute temperature (K); η: viscosity of the dispersing medium (mPa·s); $d(H)$: translational diffusion coefficient (m^2·s^{-1}).

1.5.2. Comparing DLS with double agar layer plaque assay

Several studies have shown that using DLS can offer advantages in certain aspects of phage characterization over the plaque assay. Some recent studies suggest that DLS can measure particle size distribution and aggregation kinetics much more quickly. Once standard curves are made to link changes in physical condition to changes in bioactivity, DLS is quicker, more efficient, and less damaging than plaque test (Dharmaraj et al. 2023).

The plaque assay can lead to sample loss, especially during the preparation of serial dilutions, however DLS is non-destructive and does not involve sample loss, so the same sample can be measured again and again (Clement et al. 2017). Furthermore, DLS can detect changes in particle size distribution and aggregation states, even at low concentrations, making it highly sensitive to changes in phage stability.

1.5.3. High-titer preparation of phage for DLS measurement

To obtain proper sample concentration and accurate measurement, a high-titer lysate with a high phage concentration is required. In this work, T4 lysate was prepared using the plate wash method, and PRD1 lysate was prepared using the agar culture method.

The plate wash approach and the agar culture method extract phages directly from the agar plates where they have been amplified. Initially, the host bacterial culture is mixed with a low concentration of phage and soft agar, then distributed on agar plates and incubated until plaques appear. Plates with densely packed plaques, forming a "web" pattern, yield the highest titer lysates. A completely wiped clean plate may indicate that all bacteria were destroyed before multiple rounds of infection could occur, resulting in a lower yield of titter (Skaradzińska et al., 2020).

After incubation, the phages are harvested from semi-confluent plates. The methods for harvesting phages differ between the two approaches. In the plate wash method, the phages are collected by washing the agar plate's surface with a buffer or a small amount of broth. The buffer is gently swirled over the agar surface to loosen the phages from the plaques and release them into the liquid. The mixture containing the phages is then transferred to a sterile container and centrifuged. The heavier components, such as bacterial debris and intact bacterial cells, settle at the bottom of the centrifuge tube, leaving the lighter components, such as phages and other small particles, in the supernatant. In the agar culture method, the agar surface is scraped or cut into small pieces and transferred into a buffer or LB solution. The mixture is then incubated to release the phages from the agar. Subsequent steps are similar to the plate wash method (Skaradzińska et al. 2020).

Bacteriophage storage should be long-term and stable for use in research and industrial applications. Phage lysates that are filtered and free of bacteria can be stored in screw-capped glass tubes at 4°C for months, if not years, without significant loss of infectivity. Refrigeration slows down potential degradation processes and helps maintain the structural integrity of the phage particles. However, storage at -80°C with the addition of antifreeze agents, such as glycerol, can extend stability to several years. The shelf life of phage lysates depends on the specific conditions and types of phages being stored (Fortier and Moineau 2009).
Phage lysate may include a variety of contaminants, like host cell debris, nucleic acids, proteins, and impurities. Purification helps to eliminate the impurities, ensuring that the phage sample is pure and free of interfering substances.

Bacteriophages may be easily concentrated from crude lysates of infected bacteria by adding polyethylene glycol (PEG). PEG 6000 has been found to provide optimal precipitation conditions for a variety of phages (Yamamoto et al. 1970). PEG works as a neutral solvent sponge, limiting solvent accessibility. As the concentration of PEG increases, so does the effective protein concentration until solubility is surpassed and precipitation occurs (Atha and Ingham 1981). The presence of salt enhances the precipitation of virus particles by promoting the salting-out effect of PEG. Therefore, by adding a mixture of PEG and salt, the phages aggregate and precipitate out of solution (Chan-Wha and Kyun Rha 1996). For most phages, a PEG concentration of 10% is sufficient to pellet at least 90% of their infective titer in 1 hour at 4°C. However, various phages may require varying PEG concentrations for optimal precipitation efficiency (Yamamoto et al. 1970).

PEG precipitation alone is often insufficient for preparing bacteriophage samples for DLS because it can co-precipitate contaminants such as proteins, nucleic acids, and cellular debris. This leads to a heterogeneous mixture that can cause background noise and high polydispersity, skewing the DLS results. These impurities are effectively separated and purified using (ultra)centrifugation typically with a density gradient. particularly using a sucrose or cesium chloride gradient, is a common method to separate phages based on their buoyant density (Wang et al. 2018).

1.5.4. Sample Preparation for DLS measurement

After purifying the phages, DLS can be used to study the physical properties of the phage preparations. Prepared solutions for DLS must be clear to very little blurry. Although the instrument can measure solutions at concentrations of up to 40%, and probably higher, the size measured in these conditions will be inaccurate (Farrell and Brousseau 2018).
To obtain a clear solution, the purified phages should be suspended in a suitable liquid medium. The stability of the phage particles in the solution and compatibility with the DLS apparatus should all be considered when selecting a liquid medium for DLS experiments. The liquid medium must be optically transparent and filterable, with a Refractive Index different from particles, have low viscosity, have minimal absorbance, and be compatible with the examined particles (i.e. not cause swelling, dissolution or aggregation (Farrell and Brousseau 2018).

In some cases, it is recommended to homogenize the sample with a vortex before performing DLS measurements. This helps ensure that the sample is uniformly mixed and free of aggregates, leading to more accurate and reliable results (Ruiz et al. 2022). In our studies, the purified phage solutions were vortexed before DLS measurements. However, the treated samples were not vortexed because we aimed to detect any aggregations within the samples, and vortexing could potentially impact the results.

1.6. DLS Data Analysis

1.6.1. Autocorrelation function

The correlation coefficient versus time graph is crucial for data analysis, and includes all data related to particle diffusion inside the sample ("Common Terms Used in Dynamic Light Scattering" 2013). The DLS instrument measures time fluctuations of light intensity caused by the motions of macromolecules in solution. These intensity fluctuations over time are represented by an autocorrelation function $G_2(\tau)$ (equation 2) ("Dynamic Light Scattering (AKA QLS, PCS)" n.d.). The autocorrelation function describes the correlation of light intensity fluctuations at delay time τ, where G2(τ) is the measured intensity autocorrelation function, B is a baseline constant representing the average intensity, β is a coherence factor depending on the experimental setup, and $|g_1(\tau)|^2$ is the normalized intensity autocorrelation function related to the scattered light's electric field autocorrelation.

$$G_2(\tau)=B\,[1+\beta\,|\,g^1(\tau)\,|^2] \qquad (2)$$

For a monodisperse particle dispersion, the correlation curve should be smooth and have only one exponential decay function. The y-Intercept, also known as the Intercept, is the point at where the correlation curve intersects the correlogram's y-axis. The intercept may be used to calculate the signal-to-noise ratio of a measured sample, and it is commonly used to assess data quality. It is typically scaled such

that an ideal signal yields a value of 1, whereas a good system yield intercepts greater than 0.6. ("Common Terms Used in Dynamic Light Scattering" 2013)

1.6.2. Size Distribution

DLS can measure particle sizes ranging from 1 nm to around 5 μm (Lim et al. 2013). The sizing result is represented as the z-average and size distribution, which can be in the form of intensity-weighted distribution, volume distribution, or number distribution. Each of these distributions provides unique insights into the sample's qualities.

The primary outcome of a DLS experiment is the intensity-weighted distribution of particle sizes, which indicates the relative intensity of the scattered light from particles of various sizes. According to Rayleigh's approximation, the intensity of scattered light increases with the sixth power of the particle radius ($I \propto d^6$) (Lim et al. 2013) (Malvern Instruments 2013). Thus, the intensity-weighted distribution can be misleading when a small number of aggregates or larger particles are present in the solution. These larger particles can dominate the distribution, causing the intensity-weighted distribution to inaccurately represent the overall size distribution of the sample.

The intensity-weighted distribution data can be automatically transformed into volume-weighted and number distribution data using Mie theory (Malvern Instruments Worldwide 2011). the volume distribution transforms the intensity-weighted distribution into a distribution based on particle volume, which scales with the third power of the particle radius ($V \propto r^3$). This provides a more balanced perspective of the sample by considering the volume occupied by particles of various sizes, although bigger particles are still given more weight. the number distribution depicts the actual number of particles in each size class, disregarding their scattering intensity or volume (Lim et al. 2013). Choosing the right distribution type depending on the analysis's needs is crucial, as each kind has unique biases and uses.

1.6.3. Z-average and PDI

Understanding the average size (z-average) and PDI is fundamental for interpreting DLS results. The z-average, also known as the cumulants mean, is the intensity-weighted mean hydrodynamic size of the population of particles derived from a cumulants analysis of the measured correlation curve. The z-average assumes a monodisperse sample with a Gaussian distribution.

The quantitative description of polydispersity, called polydispersity index (PDI), measures the sample's polydispersity based on its size distribution width. A PDI greater than 0.7 indicates that the sample is too polydisperse for accurate size distribution measurement. Conversely, a PDI less than 0.05 signifies a purely monodisperse sample, resulting in a monomodal distribution (Karmakar n.d.).

1.7. Phage stability

1.7.1. Stability as a variable concept among phage strains

Phages are composed of nucleic acids and proteins that may lose their function under certain physicochemical conditions. Phage stability is crucial for the effective use of bacteriophages as alternative antibacterial agents. However, phages often exhibit variable stability in solution. Therefore, phage preparations should maintain high therapeutic efficacy during treatment and maintain stable activity when exposed to unfavorable physicochemical and physiological conditions during storage (Jończyk-Matysiak et al. 2019).

The concept of stability may vary by phage strain. Some phages are considered stable if their titer does not dramatically diminish after a few days, while others may remain stable for months and years (Pirnay *et al.* 2015). Several factors can affect phage stability, including temperature, pH, ion concentration, osmolarity, storage conditions, host factors, exposure to chemicals, disinfectants, and solvents, as well as exposure to UV light or sunlight (Jończyk-Matysiak et al. 2019).

1.7.2. Effect of heat-treatment on phages

The global molecular mechanisms behind virus inactivation and the structural changes induced by heat are not fully understood (Vörös et al. 2018). Heat treatment is thought to inactivate phages by denaturing the secondary structures of proteins and other molecules, causing decreased molecular function ("Virus Inactivation Mechanisms" n.d.). loss of DNA from capsids due to heat exposure has been suggested as a possible way of inactivation, along with protein denaturation. However, little is known about the structural changes that heat induces in phages (Vörös et al. 2018).

For example, studies have demonstrated that upon heating, the tail of bacteriophage λ is first disrupted around 68°C, which triggers the release of the DNA. The head of the capsid subsequently melts at a higher temperature of around 87°C. This sequential denaturation indicates that different structural components of the phage capsid respond distinctively to thermal stress, with the tail region being more susceptible to early disruption compared to the head (Qiu 2012). Also, studies on protein denaturation indicated that thermal stress leads to the unfolding of protein structures, which is consistent with the observed behavior in phage capsid component (Jespers et al. 2004).

Another study on heating bacteriophage showed that exposing T7 particles to 65 ˚C caused the release of genomic DNA and the loss of tails, making phage particles unstable. Increasing the temperature to 80 ˚C improved mechanical stability, possibly because of the partial denaturation of the capsomeric proteins that maintain the overall capsid structure. Heat treatment resulted in DNA loss, but the T7 phage's capsid was remarkable in its ability to endure high temperatures while maintaining nearly all its global topographical structure (Vörös et al. 2018). Partial denaturation can occur within the overall structural constraints of the viral capsid.

Recent studies have shown that ion strength can affect phage inactivation temperature. Changes in ion strength influence phage stability and susceptibility to inactivation. For example, heating T4 phage at 50 to 70°C, even in extreme conditions, has shown slowed inactivation due to the presence of alkaline cations. Both single-charged and doubly charged ions had a stabilizing effect, with sodium (Na^+), potassium (K^+), and magnesium (Mg^{2+}) having the most significant impacts, while calcium (Ca^{2+}) did not (Lark and Adams 1953).

In general, the precise temperature at which a phage becomes inactive can differ from one strain of phage to another and from one protein composition to another. The proteinaceous structures of most phages can begin to suffer serious damage at temperatures exceeding 50-60°C. Rapid loss of phage infectivity occurs at temperatures greater than 70–80°C, when protein denaturation is most noticeable (Blazanin et al. 2021). Most phages can be inactivated within minutes of exposure to extreme heat, such as boiling temperatures (100°C). Phages in lysate form may sustain activity throughout storage at 4 °C, -20°C, and -80°C (Ritchie 1977). However, ice crystals at -20 °C can also potentially inactivate phages (Hatch and Warren 1969). Therefore, additional research is needed to address these concerns.

1.7.3. Effect of sonication on phages

Sonication or the act of applying ultrasonic energy to phage particles can significantly affect phage stability. Ultrasonic action works based on cavitation effect, producing heat, and reactive oxygen species (ROS) (Lu et al. 2023). The inactivation of a phage by ultrasound is dependent on several elements, including the ultrasonic power, wave amplitude, sample volume, temperature, composition, and the characteristics of the phage, such as its size, composition, and shape (Nunes et al. 2022).

The ultrasonic cavitation process uses high-frequency sound waves to produce tiny bubbles in a liquid. Rapid formation and collapse of these bubbles results in significant local temperature and pressure fluctuations. Strong shock waves and shear forces are created when these bubbles burst, and these forces have the potential to damage cellular structures. (Li et al. 2021) mechanical effects of cavitation can inactivate viruses by destroying their lipid membranes and protein spikes (Chrysikopoulos et al. 2013) with extreme pressure and heat. Cavitation can indirectly cause radical production, which may supplement mechanical stresses in viral structures ("Ultrasound–biophysics mechanisms" n.d.). Free radicals may help to inactivate viruses by oxidizing the protein capsid and DNA (Filipić et al. 2022).

1.8. The structural features of the phages T4 and PRD1

1.8.1. Bacteriophage T4

Bacteriophage T4 is the most extensively studied member of *Tevenvirinae,* subfamily of viruses in the family *Straboviridae* of class *Caudoviricetes* (Nikulin and Zimin 2021). T4 is one of the largest bacteriophages, measuring about 200 nanometers in length and 90 nanometers in width, as observed through electron microscopy (Bichet *et al.* 2021).

T4 has a prolate icosahedron (T_{mid}=20) capsid, 119.5 nm length and 86 nm width, containing 172 kg of continuous double-stranded DNA genome. The capsid comprises 930 copies of gp23, 55 copies of gp24, 12 copies of gp20, and two outer capsid proteins: Hoc (39 kDa) and Soc (Fokine et al. 2004) (Sathaliyawala et al. 2006).

The tail is made up of a sheath, an internal tail tube, and a baseplate located at its distal end. The capsid connects to a tail assembly via the neck, which is continuous with a rigid cylindrical tail tube about 94 nm long, with an exterior diameter of 9.6 nm and an interior diameter of 4.3 nm (Maghsoodi et al. 2016). The tail tube consists of gp19 protein monomers covered by a helical sheath. This sheath is composed of six helical strands, each made of 23 gp18 protein subunits that interact with one another. The strands are connected at the top of the neck and at the bottom to the baseplate. They also align side by side to form 23 groups, each containing six units (Yap and Rossmann 2014).

Six long tail fibers are attached to the baseplate's periphery and serve as the host cell recognition sensors. During an infection, both the sheath and the bottom part undergo significant structural changes (Yap and Rossmann 2014).

1.8.2. Bacteriophage PRD1

The PRD1 bacteriophage is a member of the *Tectiviridae* family, characterized by an icosahedral outer protein layer surrounding an internal lipid membrane. This membrane protects its linear, double-stranded DNA genome. PRD1 can infect specific bacteria, including *E. coli*, *S. Typhimurium*, and *Pseudomonas aeruginosa*, which possess a multidrug resistance plasmid known as *IncP*-type, carrying the phage receptor (Žiedaitė et al. 2005).

The outer protein shell of the PRD1 bacteriophage is composed of P3 trimers arranged in a pseudo-T=25 lattice and stabilized by the P30 protein. The spike-penton complex is located where proteins P2, P5, and P31 converge. Protein P2 recognizes and binds to a receptor on the host cell's membrane, triggering the formation of an opening at a capsid vertex. This leads to the membrane transforming into a tubular, tail-like structure that facilitates the entry of DNA into the host cell. Virion-associated lytic enzymes assist in transporting DNA through the peptidoglycan layer (Žiedaitė et al. 2005).

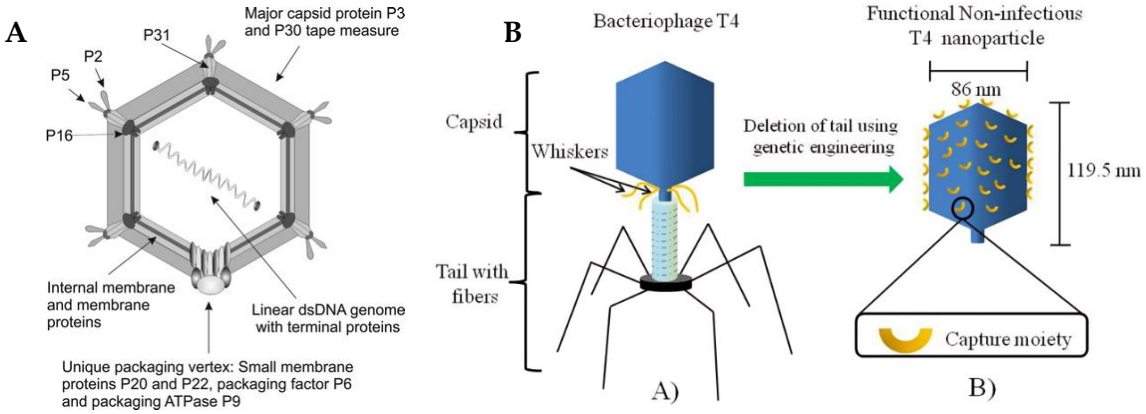

Figure 1. Schematic representation of the PRD1 (left) (Butcher *et al.* 2012) and T4 (right) (Archer and Liu 2009).

1.9. Aims of the study

The purpose of this study was to investigate the effectiveness of DLS in analyzing the physical state of T4 and PRD1 phages. The study measured the size, size distribution, and particle concentration of phage suspensions before and after treatment with heating and sonication and compared the results with plaque assay results.

Szermer-Olearnik *et al*. determined the hydrodynamic size of the T4 phage to be approximately 137.9 ± 1.06 nm (Szermer-Olearnik et al. 2017)· Accordingly, we anticipated that our measurements of the T4 phage would yield comparable results. For PRD1, which has a size of approximately 65 nm, we anticipated observing a larger hydrodynamic size due to the hydrated state of the particles typically measured by DLS. Inspired by the findings of Dharmaraj et al., we anticipated that the treated samples would exhibit polydispersity, manifested as distinct peaks or broad peaks with shoulders in the size and volume weighted distributions (Dharmaraj et al. 2023). We expected an increase in the z-average and PDI, changes in particle concentration and a decrease in phage titer in the double agar overlay plaque assay compared to the control samples.

2. MATERIALS AND METHODS

2.1. Phage strain, bacterial host, and media

The T4 and PRD1 phages, and their host bacterial strains, *E. coli* DMS616 and *S. Typhimurium serovar* DS88, were sourced from the -80°C freezer stocks at the University of Jyväskylä. The bacterial strains were cultivated in 5 ml liquid Luria-Bertani (LB) cultures and on LB plates (1% agar). Liquid cultures were incubated in an incubator shaker (New Brunswick Excella E24, Eppendorf, Hamburg, Germany) at 230 rpm and 37°C, and plates were incubated at 37°C in a CO_2 incubator. The

phage particle titer, measured in plaque-forming units (PFU) per ml, was determined using the double-layer agar method.

Polyethylene Glycol 6000 (PEG 6000) was supplied by Sigma-Aldrich, Darmstadt, Germany (CAS No. 25322-68-3), Sodium Chloride (NaCl) was purchased from VWR, Belgium (CAS No. 7647-14-5, MW 58.44), and Sucrose (D(+)-Saccharose) was purchased from VWR Chemicals, Leuven, Belgium. To create 5-20% sucrose gradient, Sucrose solutions at concentrations of 5% and 20% (w/v) were prepared using distilled water and filtered through a syringe filters. The linear sucrose gradients were formed using the Gradient former (Gradient Master 107, BioComp Instruments, USA)

20 mM potassium phosphate buffer was used for diluting phages during different steps of purification and DLS measurement. Syringe filter (Filtropur S, PES, pore size: 0.2 µm, Sartorius, Germany, Product No. 83.1826.001) was used for filtering solutions, including the buffers, phage lysates and glucose solutions to ensure sterility. Detailed information on solutions and media can be found in Appendix 1.

2.2. Phage Purification

2.2.1. Determining the titer of phage stocks using double agar overlay plaque assay

To get countable plaques, the T4 and PRD1 phage stocks were diluted in LB broth down to 10^{-10}, right before the assay. 3 ml of LB soft agar (0.7% agar) at 47 °C, 200 µl of the host culture, and 100 µl of each phage dilution were rapidly and thoroughly mixed by vortexing and poured onto an agar plate. The overlay medium was allowed to solidify by placing the dishes on a level surface at room temperature for 15 minutes, and the dishes were then incubated overnight at 37°C, in an incubator. The titers of phage stocks were calculated using equation (2). plaques (on plate 10^{-k}) represents the number of plaques observed on the plate that was diluted by a factor of 10^{-k}.

$$\text{Titer (PFU/mL)} = \text{plaques (on plate } 10^{-k}) \times 10 \times 10^{k} \quad (2)$$

2.2.2. Preparing the T4 and PRD1 lysates

Dilutions of phage suspensions mixed with bacteria were plated as described in the double agar overlay plaque assay protocol, to achieve Five semi-confluent plates of T4 and twenty semi-confluent plates of PRD1.

Following the formation of plaques, 5 ml of LB-broth was added to each T4 plate and incubated at 150 rpm and 4 °C for 2 hours using a shaker (Heidolph Hei-MIX series Vibramax 100, Heidolph Instruments GmbH & Co. KG, Germany). The plate surface was gently scraped with a z-rod and transferred to a screw-cap tube using a sterile syringe. Using a Fiberlite F21-8x50y rotor from Thermo Scientific (USA) in a Sorvall RC6+ centrifuge, the phage suspension was centrifugated at

10,000 rpm for 10 minutes at 4°C. The liquid on top was filtered using a 0.2 µm syringe filter, and the final phage stock was stored at 4 °C.

The PRD1 phages were harvested from the semi-confluent plates by gently scraping the top agar using a z-rod. The collected top agar was then transferred to an Erlenmeyer flask, and 5 ml of LB broth was added per plate. The phage suspension was incubated in the incubator shaker at 230 rpm and 37 °C for 3 hours. Following incubation, the PRD1 phage suspension was cleared through centrifugation using a Sorvall SS34 rotor at 10,000 rpm for 10 minutes at 4 °C. Prior to storage at 4 °C, the phage lysate was filtered using a 0.2 um syringe filter.

2.2.3. Phage PEG precipitation/purification

The lysates were transferred into Erlenmeyer flasks and supplemented to a final concentration of 10% PEG 6000 and 0.5 M NaCl. After incubation for 15 minutes at 4 °C, percipitaed phages were pelleted at 8000 rpm in a Sorvall RC6+ centrifuge using an SLA-1500 Rotor for 30 min at 4 °C.
T4 and PRD1 Pellets were re-suspended in 2 ml and 5 ml of 20 mM potassium phosphate buffer respectively. The suspension was centrifuged (Mega Star 1.6/1.6R, VWR International, LLC) for 5 minutes at 4000 x g and 4 °C. The supernatant was transferred to a clean Eppendorf for the second purification step.

2.2.4. Phage Purification by Sucrose Density Gradients

Sucrose solutions were made in distilled water. The PRD1 suspension was layered on gradients of 5 to 20% (w/v) sucrose and centrifuged using a SW-28 rotor in an ultracentrifuge (Optima L-100K, Beckman Coulter) at 24,000 rpm for one hour at 15 °C. The lower light scattering band was collected and phages were pelleted by ultracentrifugation for 3 hours at 33,000 rpm and 4 °C using a 70-Ti rotor. The supernatant was discarded, and the pellet (purified PRD1) was resuspended in 20 mM potassium phosphate buffer and stored on ice.

The T4 suspension was layered on gradients of 5 to 20% (w/v) sucrose and centrifuged using a SW41 rotor, at 24,000 rpm, 15°C for 20 minutes in a Beckman Coulter Optima L-100K ultra centrifuge. An additional 10 minutes of ultracentrifugation followed the initial 20 minutes for better results. The lower and upper bands were collected and centrifuged for 2 hours at 4 °C and 34 k using a 70Ti rotor, to pellet the phages. The lower pellet was resuspended in 50 µl of 20 mM potassium phosphate buffer, and the upper pellet was resuspended in 100 µl of 20 mM potassium phosphate buffer. The lower pellet suspension was labeled as "purified T4" and stored on ice.

The lower band after Sucrose density gradient ultracentrifugation is referred to as the "L-band", and the upper band is referred to as the "U-band". The pellet resulting from the centrifugation of the upper band was labeled as the "U-pellet," and the pellet resulting from the lower band centrifugation was labeled as the "L-

pellet." The titers of PEG-Pellet, L-Pellet, U-Pellet, U-Band, L-Band, and phage lysates were measured using double agar overlay plaque assay.

2.3. Bradford protein assay

The protein concentrations of the purified phages were measured using the Bradford protein assay. The Bovine serum albumin (BSA) stock solution was diluted to a concentration of 0.1 µg/µl (50 µl 2 mg/ml BSA + 950 µl buffer) using 1x phosphate-buffered saline (PBS). The 0.1 µg/µl BSA was serially diluted in PBS to yield concentrations of 0.01; 0.02; 0.03; 0.04 and 0.05 µg/µl.

The assay was performed in a total volume of 200 µL, containing 100 µL of Bradford Reagent (1X) (Table 1). The contents of all wells were mixed by pipetting and incubated at room temperature (RT) for five minutes. Following incubation, the measurement was performed using a microplate reader (Thermo Scientific Microplate Photometer, Multiskan FC, USA).

Table 1. Bradford Assay for Phage Concentration Determination. Protein (µg) represents the protein concentration in micrograms, calculated by multiplying the BSA concentration (0.1 µg/µL) by the volume of the BSA. Amount of Sample (µL) represents the volume of the original sample (protein BSA/Phage) added to the assay in microliters. Amount of Buffer (µL) represents the volume of PBS buffer added to the assay to achieve the desired dilution in microliters.

Standard/Sample	Protein (µg)	Amount of sample (µl)	Amount of buffer (µl)
Standard 1	1	10 µl BSA	90
Standard 2	2	20 µl BSA	80
Standard 3	3	30 µl BSA	70
Standard 4	4	40 µl BSA	60
Standard 5	5	50 µl BSA	50
Standard 6	0	0	100
Standard 1	unknown	10 µl T4	90
Standard 2	unknown	50 µl T4	50
Standard 3	unknown	10 µl PRD1	90
Standard 4	unknown	50 µl PRD1	50

2.4. DLS measurement

DLS measurements were carried out using a Malvern Zetasizer (Malvern Panalytical Ltd., UK). The instrument utilized Multi-Angle Dynamic Light

Scattering (MADLS) technology for the particle concentration measurements. A 10 mW He-Ne laser operating at a wavelength of 633 nm and a detection angle of 173° (backscatter) was employed for size measurements with an equilibration time of 120 sec. Two millilitre of sample was measured in a 1 cm × 1 cm transparent disposable cuvette. The temperature was controlled and maintained at 25°C during the measurements. The hydrodynamic radii (R_h) were calculated using the Stokes–Einstein equation (Equation 1).

For each sample, three size measurements were taken to ensure reproducibility, and the data were analyzed using the ZS Xplorer software (Malvern Panalytical Ltd.). Prior to measurement, samples were diluted in 20 mM potassium phosphate buffer to ensure that the scattering intensity was within the optimal range for the instrument. The average size (z-average) and polydispersity index (PDI) were calculated using the cumulants analysis method. Statistical analysis of the DLS data was conducted using Microsoft Excel (version 2020).

After each DLS measurement, the phage titer was determined using a plaque assay, as described in the double agar overlay plaque assay protocol.

2.5. Phage characterization and optimization using DLS

To find the best phage titer for DLS measurement, different dilutions of each phage were made in 20 mM potassium phosphate buffer and tested. A ten-fold serial dilution of T4 starting with an initial titer of 4.5×10^{12} was prepared up to the 10^{-5} dilution. Ten-fold serial dilutions of PRD1 were prepared up to the 10^{-4} dilution, starting with an initial titer of 8×10^{12} PFU/mL. T4 dilutions with dilution factors of 10^3, 10^4, and 10^5 and PRD1 samples with dilution factors of 10^2, 10^3, and 10^4 were measured using DLS. A separate set of purified T4 samples diluted in distilled water was prepared and stored at 4°C for three weeks to examine the phage stability in water.

2.5.1. Heat-treatment of phages

The purified phages were diluted in a 20 mM potassium phosphate buffer to achieve a titer of 7.8×10^{11} PFU/mL for PRD1 and 2.4×10^8 PFU/mL for T4. Each sample tube was securely capped to prevent evaporation or contamination during the heating process. The samples were heat-treated using a Digital Dry Bath (Labnet AccuBlock, Labnet International, Inc., Edison, USA) equipped with a block heater capable of accommodating multiple sample tubes simultaneously.

For T4, the dry bath was set to a temperature of 70°C, and samples were heated at the same temperature for varying durations of 60 minutes, 90 minutes, and 130 minutes. For PRD1, samples were heated at 70°C for 60 minutes, 90 minutes, and 120 minutes. During heating, the dry bath maintained a constant temperature with an accuracy of ±0.5°C. Control experiments were conducted in parallel, maintained at 4°C. The control samples were vortexed for one minute before measurement, while the treated samples were measured without vortexing.

2.5.2. Sonication treatment of Phages

The purified phages samples were diluted in a 20 mM potassium phosphate buffer to achieve a titer of 7.8×10^{11} PFU/mL for PRD1 and 2.4×10^{8} PFU/mL for T4. The samples were sonicated using a probe sonicator (Branson XL-2000 series, Branson Ultrasonics Corporation, Danbury, CT, USA) at an amplitude of 20% for different durations of 60 sec, 55 sec, and 10 sec with pulse cycles of 0.5:1, 1:1 and 0.5:1 second pulse (on: off) respectively, at room temperature, to find the optimal setting.

The 5 ml Eppendorf tubes, compatible with the sonicator probe and containing 2 ml sample, were placed in an ice bath to maintain a low temperature during sonication. The tubes were secured on ice to prevent the probe from touching the sides or bottom. The control samples were kept on ice without sonication.

3. RESULTS

3.1. Phage purification by PEG precipitation and sucrose gradient ultracentrifugation

The phages T4 and PRD1 were purified using standard PEG/NaCl precipitation, followed by 5-20% sucrose gradient ultracentrifugation. During ultracentrifugation, the particles migrated through the gradient, forming two distinguishable bands based on their size (Figure 2). The lower density band (upper band) presumably represented a mixture of procapsids, phage components, bacterial remnants, cell debris, and impurities, with an overabundance of capsid structures, settling near the top of the gradient. The higher density band (lower band), hypothesized to consist of intact phage particles, appeared closer to the bottom.

The T4 phages formed a bluish-white, opalescent band, while the PRD1 phages formed a clear, transparent band. For both phages, the upper band was less dense, and fainter compared to the lower band. Gradient-purified phage preparations were collected and further purified by centrifugation.

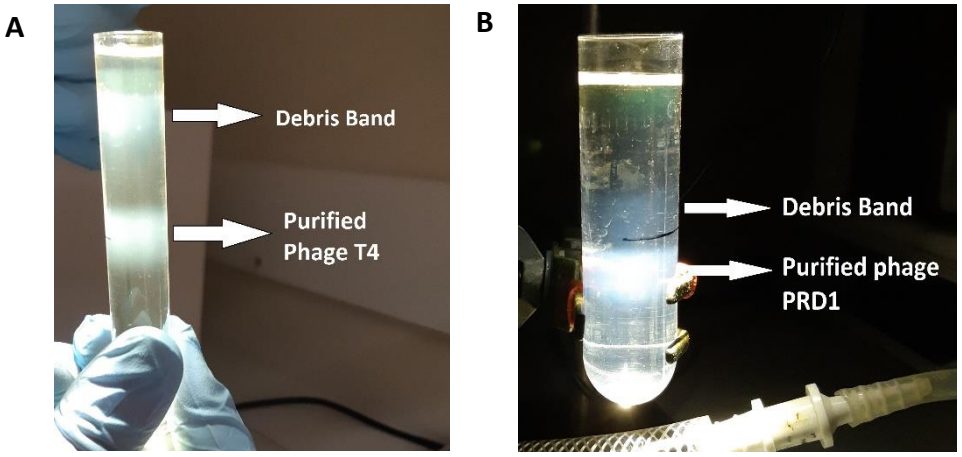

Figure 2. Purification of phages T4 and PRD1 using 5-20% sucrose gradients resulted in distinct bands. Bacteriophages harvested after precipitation with PEG were layered over a sucrose step gradient.

3.2. Bradford test

The Bradford test was conducted to determine the protein concentration in purified phage samples at the same concentration optimized for DLS measurement. The concentration of phage (in µg/µl) was determined using the equation y = 0.1723x + 0.5045 with an R^2 value of 0.9761, where y is absorbance and x is concentration.
The protein concentration of the 10000-fold dilution of T4 (Initial titer: 2.4×10^8 PFU/mL), was 0.027 µg/µl. The protein concentration of 1000-fold dilution phage PRD1 (initial titer 7.8×10^{11} PFU/mL), was 0.021 µg/µl. Thus, the results of the Bradford test showed that a protein concentration of 0.021 µg/µl for PRD1 and 0.027 µg/µl for T4 are suitable for measurement with DLS.

3.3. Characterizing T4 Phage with DLS

3.3.1. DLS can measure the hydrodynamic size of T4 phages

To find the optimal T4 concentration for the DLS measurement, ten-fold serial dilutions of purified T4 up to the 10^{-5} dilution were prepared and measured using DLS five days after purification. The samples, with titers of 1.5×10^9, 2.4×10^8, and 1.8×10^7 PFU/mL, had intercepts of 0.98, 0.92, and 0.52, and z-average of 155, 150.6, and 147.8 nm, respectively (Figure 4.A) (Table 3). Considering the intercept values and the correlation curves, the optimal phage titer for DLS measurement was determined to be 2.4×10^8 PFU/mL.
For the optimal T4 preparation, the autocorrelation curves exhibited a smooth, exponential decay from a high initial value to zero, without multiple peaks or irregularities. The mode peak for the intensity-weighted distribution was located at 146.1 nm, indicating the hydrodynamic size of intact T4 phage particles. The volume distribution showed peak1 at 108 nm and a non-Gaussian distribution with a shoulder around 197 nm (Figure 4.B). Considering that transformations from intensity-weighted to volume distributions can amplify errors and noise, and since the volume distribution peak1 is located at sizes smaller than intact phage particles, it can be concluded that the volume distribution results are not reliable in this case, and the intensity-weighted distribution provides the most reliable size distribution.

Table 3. T4 Characterization Results.

Characterization results of phage T4 using DLS and titration. Z-average represents the intensity-weighted mean hydrodynamic size of the ensemble collection of particles nanometers. The Polydispersity Index (PDI) indicates the uniformity of particle sizes within each sample. Particle concentration (particles/ml) denotes the number of particles per milliliter of the sample, while the titer (PFU/mL) represents the titer of phages in plaque-forming units per milliliter. The samples labeled as L-pellet and U-pellet were obtained through centrifugation of the lower and upper bands, respectively, during the purification process. The T4 lysate (unpurified) sample represents the initial unprocessed T4 solution.

Sample (dilution factor)	Z-average (nm)	Intercept	PDI	Peak 1 (nm)	Peak 2 (nm)	Particle concentration (paticles/ml)	Phage titer (pfu/ml)
PEG-Pellet	N/A	N/A	N/A	N/A	N/A	N/A	3.5×10^{11}
L-Band	N/A	N/A	N/A	N/A	N/A	N/A	9.4×10^{9}
L-Pellet	N/A	N/A	N/A	N/A	N/A	N/A	4.5×10^{12}
L-Pellet (10^{-3})	155	0.98	0.22	146.1	5468	4.89×10^{9}	1.5×10^{9}
L -Pellet (10^{-4})	150.6	0.92	0.19	146.1	5468	7.12×10^{8}	2.4×10^{8}
L -Pellet (10^{-5})	147.8	0.56	0.24	146.1	5468	5.56×10^{7}	1.8×10^{7}
T4 lysate	480 ml	N/A	N/A	N/A	N/A	N/A	7.6×10^{9}
Lysate (10^{-1})	123.8	0.98	0.22	146.1	0	1.62×10^{10}	2×10^{9}
Lysate (10^{-2})	117	0.95	0.22	125.6	0	2.08×10^{9}	1.8×10^{8}
Lysate (10^{-3})	117	0.81	0.19	125.6	0	3.27×10^{8}	2.1×10^{7}
U-Band	N/A	N/A	N/A	N/A	N/A	N/A	4×10^{7}
U- Pellet	N/A	N/A	N/A	N/A	N/A	N/A	3.8×10^{9}
U-Pellet (10^{-3})	108.5	0.91	0.09	108	0	N/A	N/A
U-Pellet (10^{-4})	131.3	0.67	0.18	146.1	0	N/A	N/A
U-Pellet (10^{-5})	173.2	0.20	0.10	169.9	0	N/A	N/A

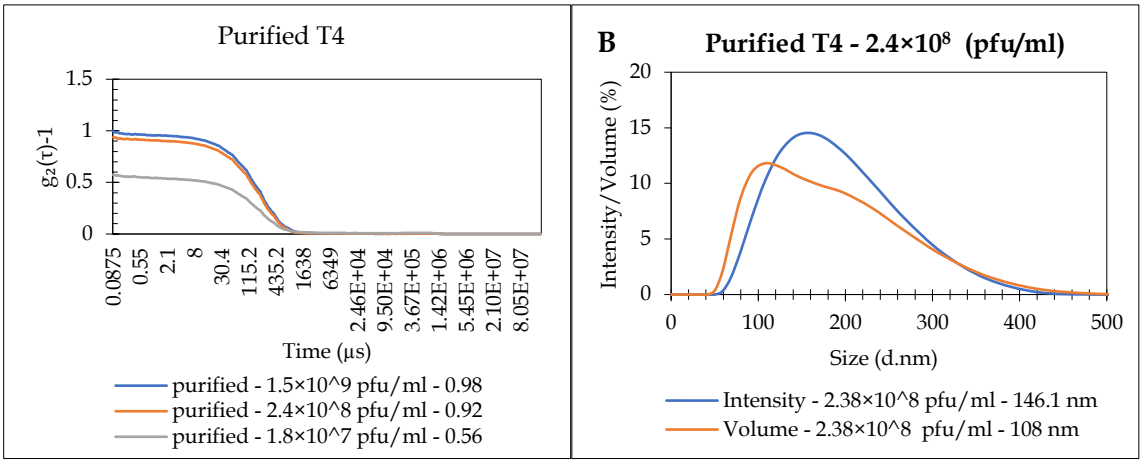

Figure 4. A) The DLS autocorrelation function (ACF) curves were measured for T4 dilutions with titers of 1.5×10^9, 2.4×10^8, and 1.8×10^7 PFU/mL. B) The intensity-weighted and volume-weighted distributions of T4 phage with a titer of 2.4×10^8 PFU/mL.

3.3.2. Volume Distribution: A Better Representation of T4 Lysate Heterogeneity

Ten-fold serial dilutions of T4 lysate were prepared up to the 10^{-3} dilution, with phage titers of 2×10^9, 1.8×10^8, and 2.1×10^7 PFU/mL, and measured by DLS, resulting in intercept values of 0.98, 0.95, and 0.81, respectiv
ely. The autocorrelation curves displayed a smooth, exponential decay from a high initial value to zero, without multiple peaks or irregularities. Therefore, all measurements were considered reliable (Figure 5.A).

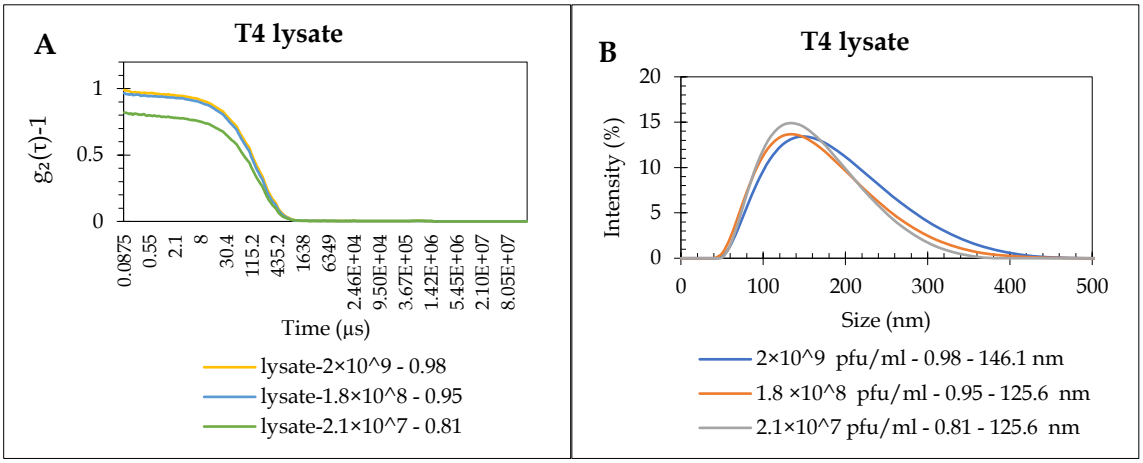

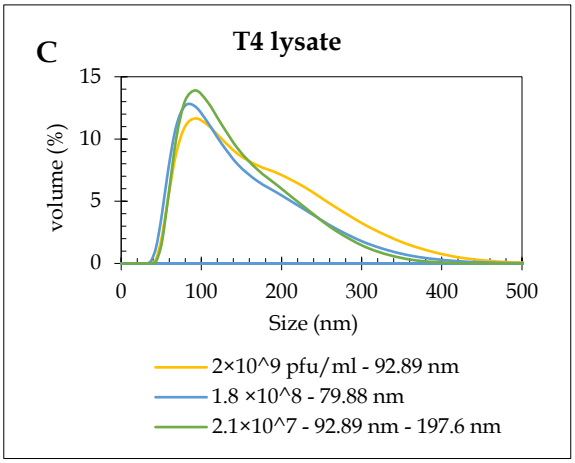

Figure 5. DLS measurement for T4 lysate preparation (titers: 2×10^9, 1.8×10^8, 2.1×10^7 PFU/mL). A) The DLS autocorrelation function (ACF) curves show smooth, exponential decay with intercepts above 0.8. B) The intensity-weighted distribution and C) the volume-weighted distribution show shoulders, indicating polydispersity.

For lysates with titers of 2×10^9, 1.8×10^8 and 2.1×10^7 PFU/mL, the mode peak for the intensity-weighted distribution was located at 146.1 nm, 125.6 nm, and 125.6 nm, respectively (Table 4), while the mode peak for the volume distribution were at 92.89 nm, 79.88 nm, and 92.89 nm (Figure 5.B and 5.C). The volume-weighted distributions exhibited a shoulder, indicating a polydisperse sample with multiple size components. This shoulder alongside the main peak is caused by the presence of larger particles or aggregates. Phage lysate is heterogeneous because it contains a mixture of phage particles, host cell debris, DNA, proteins, and residual medium components. Therefore, the volume distribution offered a more realistic view of the sample's overall heterogeneity.

The particle concentration measurements by DLS for both purified phage samples and lysates indicated that a tenfold dilution results in a tenfold reduction in both phage titer and particle concentration (Table 3).

3.3.3. Heat-treatment of T4 at 70°C causes aggregation, fragmentation and loss of infectivity

The effect of heat treatment on T4 phages was investigated in two experiments. The first experiment aimed to determine the optimal temperature for the heat treatment experiment. Two samples of T4 were prepared at a concentration of 1.5×10^8 PFU/mL. The control was kept at 4 °C, and the other sample was heated at 70 °C for 60 minutes. DLS was used to analyze the size distribution and particle

concentration of control and heated samples. The intensity-weighted size distribution of the control sample exhibited a Gaussian peak at 146.1 nm. The heated sample displayed three distinct peaks at 68.69 nm, 79.88 nm, and 169.9 nm (Figure 6.B). The z-average of the control was 180.8 nm, which increased to 480 nm after heating, and the particle concentration decreased from 2.9×10^8 PFU/mL to 1.98×10^7 PFU/mL. After heating, the plaque assay results also showed a decrease in phage titer from 1.5×10^8 to 7×10^4 PFU/mL (Table 4). The control had an intercept of 0.87, suggesting high measurement quality, whereas the heat-treated sample had an intercept of 0.52, indicating low data quality (Figure 6.A). The decreased intercept value, along with
an approximately threefold increase in z-average, the appearance of multiple peaks, reduced titer, and a tenfold decrease in particle concentration after heating, all suggest phage aggregation through the heating process.

In the second heat treatment experiment, four samples of T4 were prepared at a concentration of 6.2×10^7 PFU/mL. One sample was used as a control, and three were heated at 70 °C for 60, 90, and 130 minutes. After the initial heating and DLS measurement, treated samples were further heated until they reached a total heating time of 130 minutes, followed by another DLS measurement. The aim was to gather triple results of 130 min heated samples.

The control sample displayed an intercept of 0.87, suggesting reliable measurements. All three heated samples exhibited low intercept values (<0.6), suggesting poor data quality (Figure 6.D). The intensity-weighted distribution of the control sample showed a single sharp peak at 146.1 nm, indicating that the most abundant particles present in the sample were intact phage particles. The heated samples showed peaks at larger sizes (197.6 nm and 229.8 nm) and smaller sizes (37.56 nm and 59.07 nm) compared to intact phage particles (Figure 6.E and 6.F). The measured diameter of the treated samples particles may not be reliable due to the low intercept values. In the volume size distribution, the control sample exhibited a peak at 108 nm with a shoulder, suggesting polydispersity. All heat-treated samples exhibited broader peaks, and starting from 90 °C, changes in the curve shape and the emergence of new peaks indicated an enhanced polydispersity (Figure 6.G and 6H).

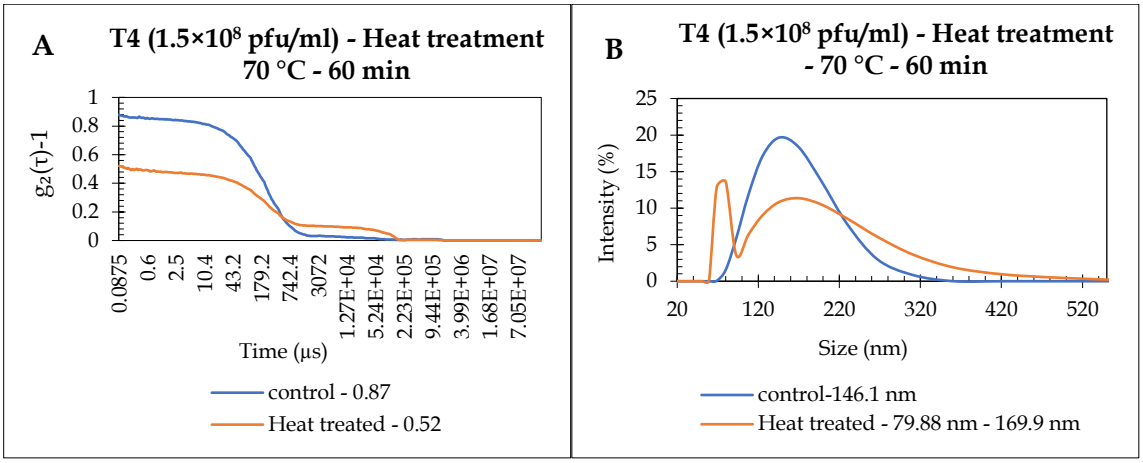

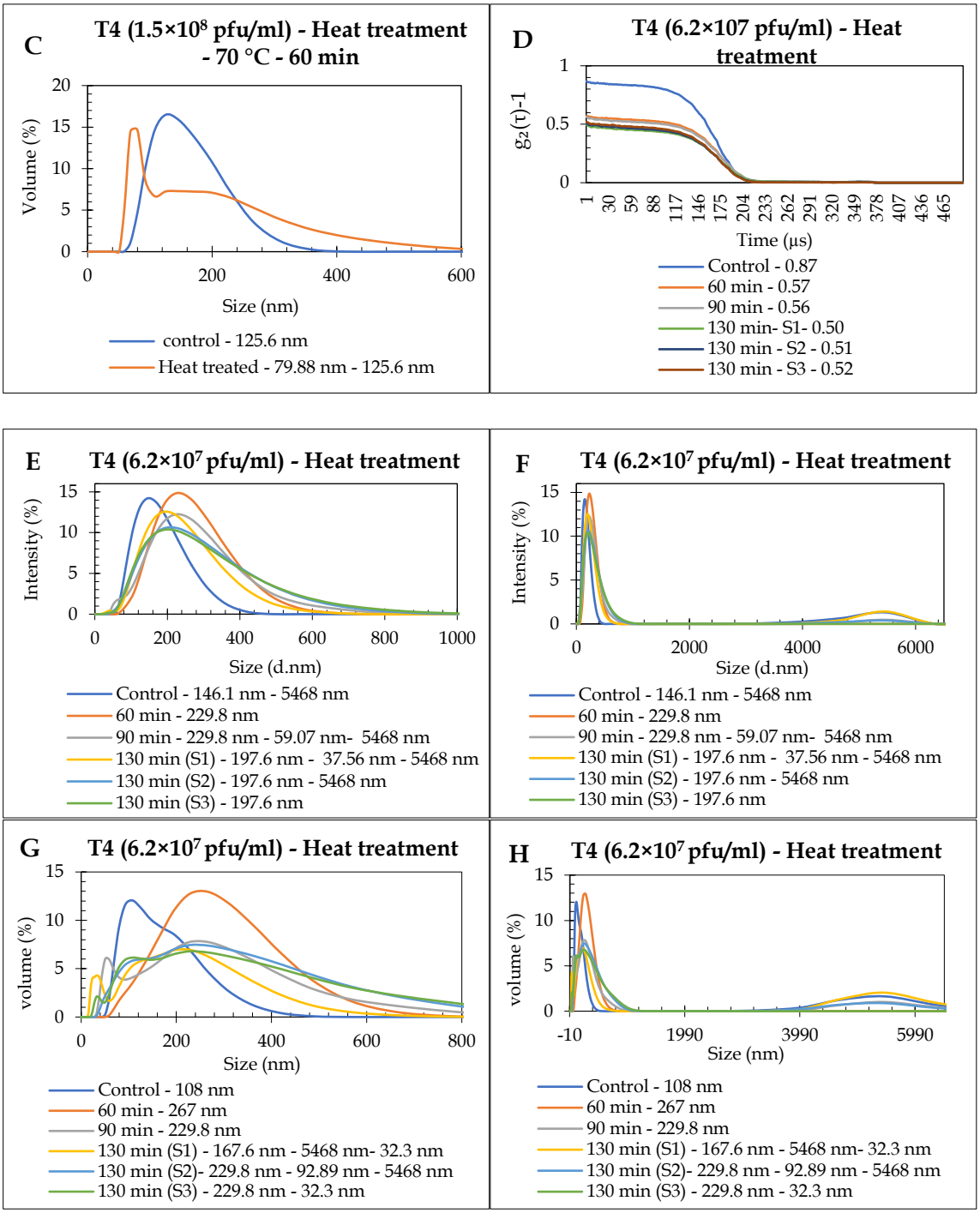

Figure 6. Experiment 1. Heat Treatment of T4 Phages (initial titer: 1.5×10^8 PFU/mL). A) DLS autocorrelation function (ACF) curves were measured for the control and heat treatment at 70 °C for 60 min. B & C) Intensity-weighted and volume-weighted distributions for the control and heat-treated samples.
Experiment 2. Heat Treatment of T4 Phages (initial titer: 6.2×10^7 PFU/mL). D) DLS ACF curves were measured for heat treatment of T4 phages (6.2×10^7 PFU/mL) at 70 °C for 60 min, 90 min, and 130 min. E & F) Intensity-weighted distributions of control and heat-treated samples. G & H) Volume-weighted distributions of control and heat-treated T4 samples. Aggregations around 5468 nm are observed in all samples.

Aggregations around 5468 nm were observed in both the control and heat-treated samples in both intensity-weighted and volume distribution profiles. As these measurements were taken 16 days after phage purification, it is possible that some aggregation occurred during storage or sample preparation.

After heating for 130 minutes, the particle concentration decreased tenfold; it was 1.11×10^8 particles/ml in the control sample and 8.1×10^7, 4.2×10^7, and 4.3×10^7 particles/ml in the heated samples, it suggests aggregation. The plaque assay indicated that the phage titers dropped to zero (Table 4).

Table 4. DLS results for the heat treatment of purified T4 phage at 70 °C. The z-average (nm) indicates the mean hydrodynamic diameter of particles in the sample. The Polydispersity Index (PDI) reflects the sample's dispersity, with lower values suggesting greater uniformity. Particle concentration (particles/mL) represents the number of particles per milliliter as measured by DLS. The titer (PFU/mL) denotes the concentration of viable phage particles, measured in plaque-forming units per milliliter.

Sample	Z-average (nm)	PDI	Intercept	Peak 1 (nm)	Peak 2 (nm)	Particle concentration (paticles/ml)	Phage titer (pfu/ml)
First Experiment							
Control	180.8	0.30	0.87	146.1	-	2.9×10^8	1.5×10^8
60 min	480	0.39	0.52	68.69	79.88	1.979×10^7	7×10^4
Second experiment							
Control	156	0.25	0.87	146.1	5468	1.11×10^8	6.2×10^7
60min	201.7	0.20	0.57	267.2	0	N/A	N/A
90 min	200	0.31	0.56	229.8	5468	N/A	N/A
130 min (S1)	193.7	0.30	0.50	197.6	5468	8.10×10^7	0
130 min (S2)	181.9	0.26	0.51	197.6	5468	4.20×10^7	0
130 min (S3)	177.8	0.24	0.52	197.6	32.3	4.26×10^7	0

3.3.4. Sonication Disrupts T4 Phage Structure and Increases Aggregation

Four samples of T4 were prepared at a concentration of 1.26×10^8 PFU/mL. One was kept at 4 °C as a control, and three samples (S1, S2, and S3) were subjected to mechanical pressure using a probe sonicator. All three samples were sonicated at an amplitude of 20% but for different durations and pulse cycles. S1 was sonicated for 1 minute (0.5 sec on/1 sec off), S2 for 55 seconds (1 sec on/1 sec off), and S3 for 10 seconds (0.5 sec on/1 sec off), all at room temperature. After sonication, the z-average values for S1, S2, and S3 were 3640 nm, 4264 nm, and 3535 nm, respectively (table 5). This indicates an approximately 25-fold increase compared to intact phage particles, suggesting potential aggregation.

The control sample had an intercept of 0.87, while the sonicated samples showed intercepts higher than one (S1: 4.21; S2: 3.93; S3: 3.27), indicating poor data quality and potential structural changes (Figure 6.A). The high intercept values suggest "number fluctuations," possibly due to aggregation or other changes induced by sonication. The intensity- and volume distribution profiles of the sonicated samples show either two distinct peaks or a broad peak, below 100 nm, significantly smaller than intact T4 phages (Figure 7.B and 7.C). The particle concentrations for S1, S2, and S3 were 6.7×10^8, 7.8×10^{10}, and 1.7×10^{10} particles/ml, respectively (table 5), suggest that the particle concentration increased in S2 and S3, supporting the hypothesis that sonication may have caused the breakdown of some phage particles.

In summary, the increase in z-average and intercept values, the appearance of multiple peaks in size distribution, and increased particle concentration underscore the significant impact of sonication on T4 phage structure.

In the second experiment, three samples of T4 were prepared at a titer of 1.26×10^8 PFU/mL and labeled as control, S1, and S2. Using a probe sonicator on ice, S1 received a 1:1 second pulse (on:off) for 10 seconds, repeated twice with a 10-second interval. S2 received the same pulse for 10 seconds, repeated three times with a 10-second interval between sonication. The control sample shows an intercept of 0.86, suggesting reliable measurement. However, the sonicated samples S1 and S2 exhibited intercepts of 2.76 and 3.51, suggesting 'number fluctuations' due to potential aggregation or structural changes likely resulting from the disruptive effects on phage structures (Figure 7.D).

The mode peak of the control sample for the intensity-weighted distribution was located at 169.9 nm (Figure 7.E), which is larger than the size of intact T4 particles. Sonication was performed 15 days after phage purification, likely resulting in some aggregations forming during the two weeks of storage in the cold room. Since the intensity-weighted distribution is sensitive to larger particles, the mode is shifted to the size of these aggregates. The mode peak of the control sample for the volume-weighted distribution was located at 146.1 nm (Figure 7.F), likely because the effect of aggregates in the volume-weight distribution is less than the intensity-weight distribution.

In the sonicated samples of both intensity and volume distribution, multiple peaks at 59.07 nm, 108 nm, and 169 nm appeared (Figure 7.E and 7.F). The z-average for the control sample was 174.4 nm, while sonication significantly increased the z-average to 2866 nm and 3313 nm. The particle concentration in S1 and S2 increased

tenfold, from 2.31×10^8 particles/ml in the control to 2.23×10^9 particles/ml for S1 and 1.54×10^9 particles/ml for S2. The phage titer decreased tenfold, from 1.26×10^8 PFU/mL in the control to 5.6×10^7 PFU/mL for S1 and 1.5×10^7 PFU/mL for S2.

These findings suggest that most of the phages were initially intact and uniformly distributed but probably disintegrated into smaller particles and large aggregates in both sonicated samples due to the mechanical force of sonication. These results underscore the effectiveness of DLS for assessing the physical state of phages.

Table 5. DLS measurements for sonicated T4 phage samples at 20% amplitude

Sample	Pulse cycle sec (on:off)	Time (sec)	Z-average (nm)	PDI	Intercept	Particle concentation (paticles/ml)	Phage titer (pfu/ml)
Control	1:1	N/A	174.4	0.31	0.86	2.31×10^8	1.26×10^8
First experiment							
S1	0.5: 1	60	3640	1	4.22	6.7×10^8	N/A
S2	1: 1	55	4264	1	3.94	7.8×10^{10}	N/A
S3	0.5: 1	10	3535	1	3.27	1.7×10^{10}	N/A
Second experiment							
10sec (2x)	1:1	60	2866	1	2.76	2.23×10^9	5.6×10^7
10 sec (3x)	1:1	60	3313	1	3.51	1.54×10^9	1.5×10^7

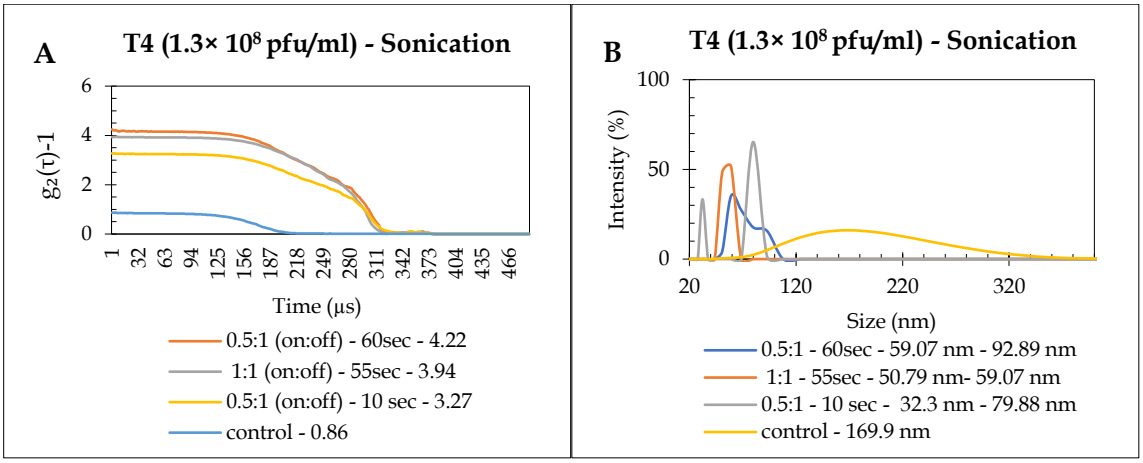

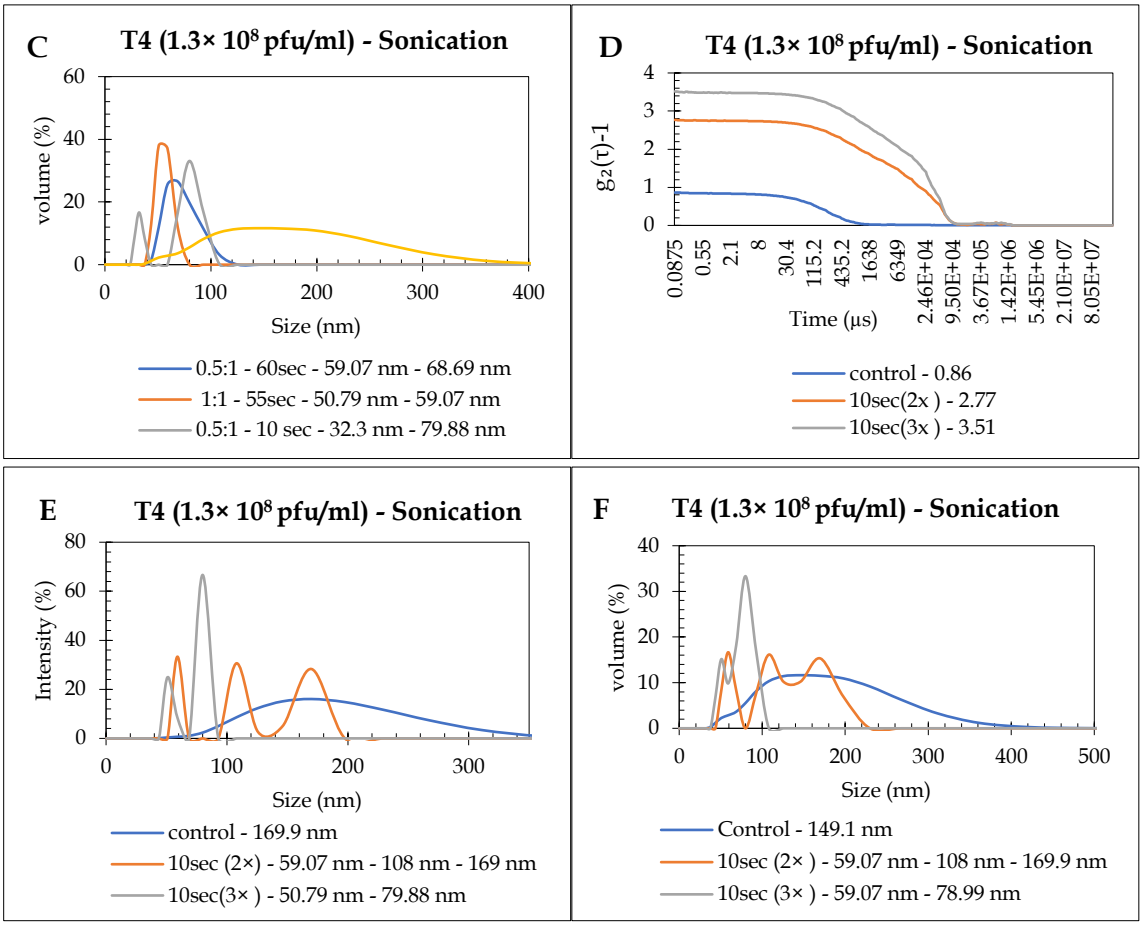

Figure 7. Sonication of T4 phages (Initila titer: 1.26×10^8 PFU/mL) at 20% amplitude. Experiment 1. Sonication of phage samples S1 (1 min, 0.5:1 sec pulse), S2 (55 sec, 1:1 sec pulse), and S3 (10 sec, 0.5:1 sec pulse). A) Autocorrelation function (ACF) curves. B & C) Intensity-weighted and volume-weighted distributions. Experiment 2. Sonication of phage samples using a 1:1 sec pulse. S1 (two 10-second sonication with a 10-second interval). S2 (three 10-second sonication with the same interval). D) Autocorrelation function (ACF) curves. E & F) Intensity-weighted and volume-weighted distributions.

3.3.5. Dilution in Water Reduces T4 Phage Stability and Promotes Aggregation

Two samples of purified T4 phage with an initial titer of 4.5×10^{12} PFU/mL were prepared with dilution factors of 10^3 and 10^4 in distilled water and stored at 4°C for three weeks. The plaque assay was not performed; the results are reported based on dilution factors to compare the size distribution and particle concentration between the freshly diluted phages in 20 mM potassium phosphate buffer and the three-week-old, diluted samples in distilled water.

The intercepts for all measured samples were higher than 0.9, suggesting reliable measurements (Figure 8.A). The fresh phage preparation diluted in buffer with a dilution factor of 10^3 had an z-average of 155 nm, with the mode peak at 146.1 nm. The phage preparation with the same dilution factor but stored in distilled

water for three weeks had an z-average of 280.6 nm and a mode peak at 108 nm. The particle concentration decreased approximately tenfold, from 4.89×10^9 to 1.52×10^8 PFU/mL in the water diluted sample (Table 6).

The fresh diluted phage in buffer with a dilution factor of 10^4, had an z-average of 150.6 nm, with the mode peak at 146.1 nm. However, the diluted phage in water showed an z-average of 272.1 nm and the mode peak was located at 310.1 nm. Particle concentration also decreased approximately tenfold, from 7.12×10^8 to 9.73×10^7 PFU/mL. The intensity-weighted size distribution indicates that fresh phages have a sharp peak at 146.1 nm, suggesting predominantly intact phage particles. In contrast, the phages diluted in water after three weeks exhibit broad peaks at 488.7 nm and 310.7 nm and shoulders at 79.88 nm, indicating increased polydispersity (Figure 8.B). The volume-weighted distribution graph shows similar results; however, the smaller particles, instead of appearing as shoulders, are appearing as a distinct peak at 68.69 nm (Figure 8.C).

These findings indicate that the stability of phages in water at 4 °C decreases with higher dilution factors, resulting in both clumping and breakdown. Phages are known to have low stability in distilled water because direct oxidation can damage the capsid and tail, leading to the loss of genetic information. This highlights the importance of storing phages correctly to maintain their integrity for different applications.

Table 6. DLS measurement results for purified T4 phages diluted in distilled water after three weeks

Dilution factor	Z-Average (nm)	PDI	Intercept	Peak 1 (nm)	Particle concentration (particles/ml)	Phage titer (pfu/ml)
Fresh purified T4 in buffer						
10^3	155	0.22	0.98	146.1	4.89×10^9	1.5×10^9
10^4	150.6	0.19	0.92	146.1	7.12×10^8	2.4×10^8
Purified T4 in distilled water after three weeks						
10^3	280.6	0.45	0.99	108	1.51×10^8	N/A
10^4	272.1	0.47	0.97	310.07	9.73×10^7	N/A

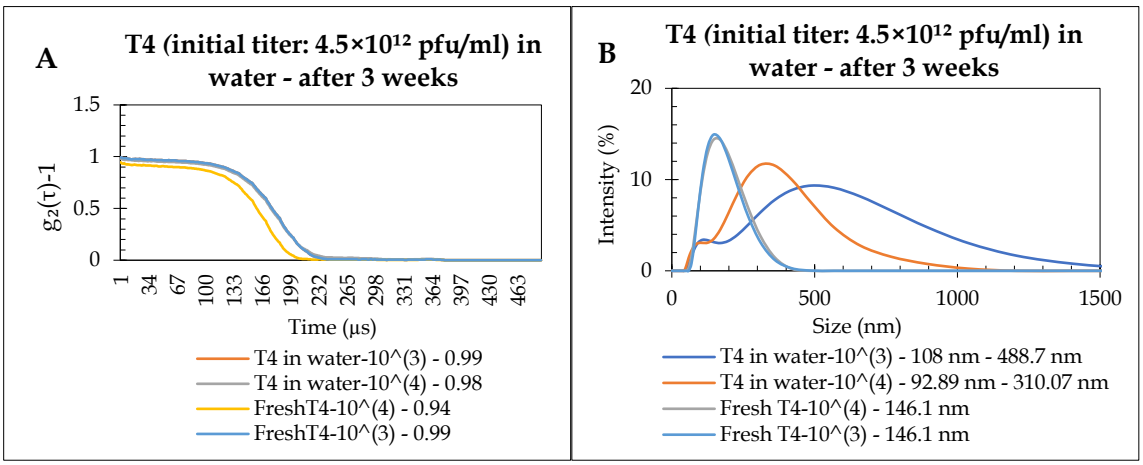

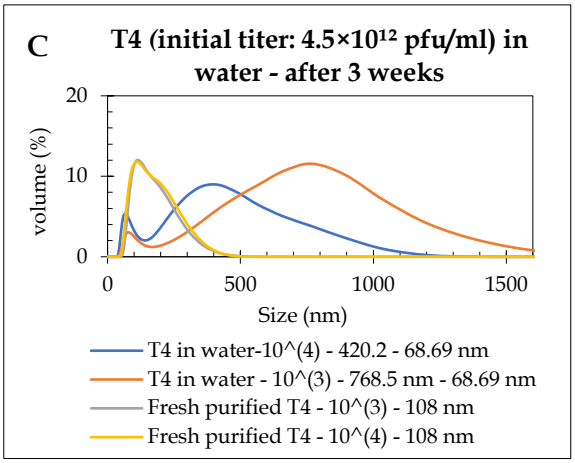

Figure 8. DLS measurement of T4 phages (initial titer: 4.5×10^{12} PFU/ml), diluted (1:1000 and 1:10000) in distilled water and stored at 4°C for three weeks, compared with fresh phage preparations in buffer. A) The DLS autocorrelation function (ACF) curves. B&C) DLS measurements of size dispersion of T4 phages diluted in water represent data weighted by intensity (B) and volume (C) of particles.

3.4. Characterizing the tailless PRD1 Phage with DLS

3.4.1. DLS can measure the hydrodynamic size of PRD1

Ten-fold serial dilutions of PRD1 were prepared up to the 10^{-5} dilution and measured using DLS five days after purification. The samples, with titers of 4.3×10^{11}, 7.8×10^{11}, and 4.7×10^{10} PFU/mL, had intercepts of 0.94, 0.94, and 0.46, and z-averages of 77.11, 78.4, and 130 nm, respectively (Table 7). The autocorrelation function showed that samples with the 7.8×10^{11} and 4.3×10^{11} PFU/mL phage titers had smooth autocorrelation curves with exponential decay, without multiple peaks or irregularities, and with intercepts close to 1, suggesting high-quality data (Figure 9.A).

The phage titer of 7.8×10^{11} PFU/mL was selected as optimal concentration for the next experiments. Th z-average for this concentration was 78.4 nm. The intensity distribution exhibited a sharp Gaussian peak at 79.88 nm, indicating that the hydrodynamic size of the complete PRD1 phages is 79.88 nm.

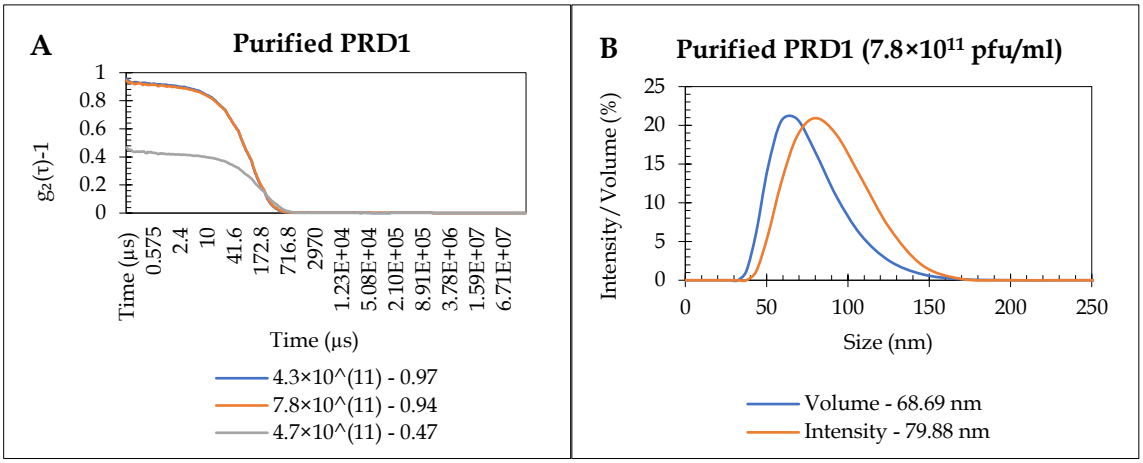

Figure 9. A) The DLS autocorrelation function (ACF) curves were measured for PRD1 dilutions with titers of 7.8×10^{11}, 4.3×10^{11}, and 4.7×10^{11} PFU/mL. B) The intensity-weighted and volume-weighted distributions of PRD1 phage with a titer of 7.8×10^{11} PFU/mL .

Table 7. PRD1 Characterization

Sample (dilution factor)	Z-average (nm)	Intercept	PDI	Peak 1 (nm)	Particle concentration (particles/ml)	Phage titer (pfu/ml)
Lysate	N/A	N/A	N/A	N/A	N/A	5.4×10^{11}
Lysate (10^1)	110.9	0.97	0.1781	125.6	2.68×10^{10}	N/A
Lysate (10^2)	113	0.97	0.1692	125.6	7.97×10^{9}	N/A
Lysate (10^3)	123.2	0.85	0.2065	146.1	2.17×10^{7}	N/A
L-Pellet	N/A	N/A	N/A	N/A	N/A	8×10^{12}
L- Pellet (10^2)	77.11	0.94	0.02	79.88	2.35×10^{10}	4.3×10^{11}
L- Pellet (10^3)	78.4	0.94	0.05	79.88	1.42×10^{10}	7.8×10^{11}
L- Pellet (10^4)	130	0.46	0.13	146.1	1.69×10^{9}	4.7×10^{10}

3.4.2. Volume Distribution: A Better Representation of PRD1 Lysate Heterogeneity

Ten-fold serial dilutions of PRD1 lysate were prepared up to the 10^{-3} dilution, starting with an initial titer of 8×10^{12} pfu/ml, and were analysed using DLS. The

autocorrelation function indicated that all samples had an intercept above 0.8, suggesting reliable measurements (Figure 10.A). The mode peak of lysates with dilution factors of 10^1, 10^2, and 10^3 for the intensity-based distribution were located at 125.6 nm, 126.6 nm, and 146.1 nm, respectively. Since these peaks are nearly double the size of intact PRD1 phage particles, they likely represent aggregates or other large particles in the lysates. Additionally, the broader peaks of lysate compared to purified phage samples indicate polydispersity in the lysate (Figure 10.B). The poly dispersity is more evident in the volume-weighted distribution, where the mode peak for dilution factors of 10^1, 10^2, and 10^3 appear at 68.69 nm, 79.88 nm, and 68.69 nm, representing intact PRD1 phage particles, with a shoulder around 197 nm, and a 23.88 nm peak for the 10^{-1} diluted sample. The volume-weighted distribution provides a more realistic profile of the size distribution due to the lysate's heterogeneity and polydispersity (Figure 10.C).

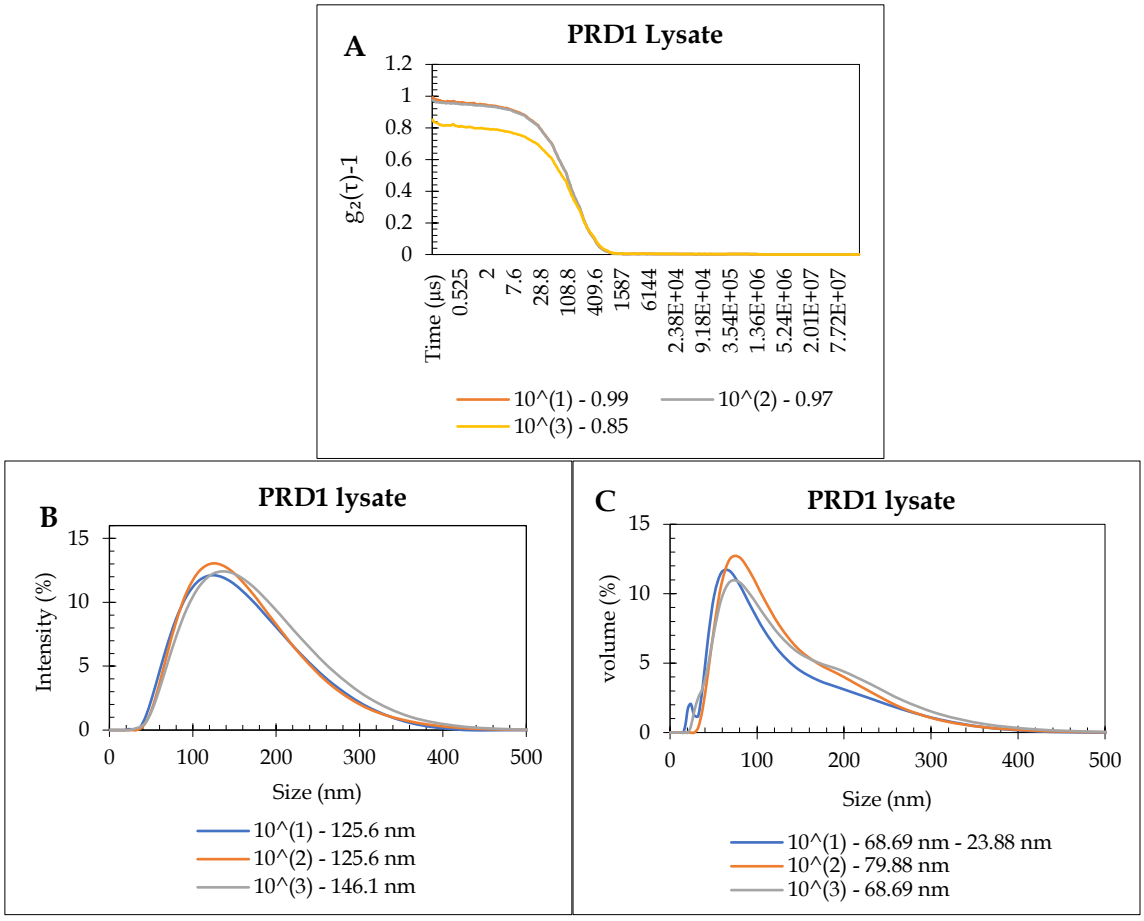

Figure 10. DLS measurements of size dispersion of PRD1 lysate. A) The DLS autocorrelation function (ACF) curves were measured for dilutions of PRD1 lysates, with an initial titer of 5.4×10^{11} pfu/ml, and dilution factors of 10^1, 10^2 and 10^3. B&C) The intensity-weighted and volume-weighted distribution show broad peaks, highlighting lysate polydispersity.

3.4.3. Impact of Heat Treatment on PRD1: Reduced Infectivity and Increased Aggregation

Four samples of PRD1 were prepared at a concentration of 7.4×10^9pfu/ml. One sample was used as the control and the remaining three samples were treated at 70°C for 60, 90, and 120 minutes. The intercept for the control sample was 0.86, suggesting high-quality data. The intercepts for the samples heat-treated for 60, 90, and 120 minutes were 0.56, 0.48, and 0.43, respectively. They were all below 0.6, suggesting low quality measurement, probably because of the polydispersity (Figure11.A).

The mode peak of the control sample for the intensity-weighted distribution was located in 79.88 nm, representing the hydrodynamic size of intact PRD1phages. However, broad peaks were observed in the samples heated for 60, 90, and 120 minutes at 79.88, 125.6, and 92.89, respectively. A peak at 5468 nm was also observed in all the heated samples. The width of the mode peaks in the heated samples was almost twice that of the control sample, indicating an increase in polydispersity due to heating (Figure11.B). However, the measured hydrodynamic sizes of the particles in the heated samples may not be reliable because the samples were not homogeneous, making the size measurement inaccurate.

The mode peak of the control sample for the volume-weighted distribution was located in 59.07 nm, which is smaller than the hydrodynamic size of intact phage particles. All heated samples exhibited three distinct broad peaks with significantly lower volume percentages compared to the control. This indicates that polydispersity increased after heating (Figure 11.C).

The phage titer in the control sample was 7.4×10^9 pfu/ml. However, after 60 minutes of heating, it decreased to 7.15×10^6 pfu/ml. The phage titer remained almost constant up to 120 minutes of heating. The particle concentration detected by DLS increased from 8.53×10^9 to 1.54×10^{10} after 60 minutes of heating. After 90 and 120 minutes of heating, it decreased by approximately 100-fold to 5×10^8 and 2.45×10^8 (Table 8). The fluctuation in particle concentration suggests that after 60 minutes of heating, some phages might have fragmented, resulting in an increased particle concentration. However, with extended heating time, aggregation may have occurred, and the particle concentration decreased to about one-tenth of the initial concentration. This is consistent with the results shown in the volume-weighted distribution chart, as the 60-minute heated sample showed two distinct peaks smaller than the control peak, supporting the fragmentation hypothesis. In contrast, the 90 and 120-minute heated samples showed a reduction from three peaks to two, reinforcing the aggregation idea.

The results from the plaque assay align with the DLS results, as DLS data indicates physical changes in the particles after 60 minutes of heating, and the plaque test results show a 1000-fold decrease in viable phage concentration.

Table 8. Results of DLS measurement for heat-treated PRD1 phage

Sample	Z-average (nm)	Intercept	PDI	Peak 1 (nm)	Peak 2 (nm)	Particle concentration (particles/ml)	Titer (pfu/ml)
Control 1	81.54	0.86	0.09708	79.88	0	8.53×10^{9}	7.4×10^{9}
60 min	85.34	0.56	0.3042	79.88	5468	1.54×10^{10}	7.1×10^{6}
90 min	114.1	0.48	0.2926	125.6	5468	5×10^{8}	7.4×10^{6}
120 min	85.73	0.43	0.2683	92.89	5468	2.45×10^{8}	5.5×10^{6}

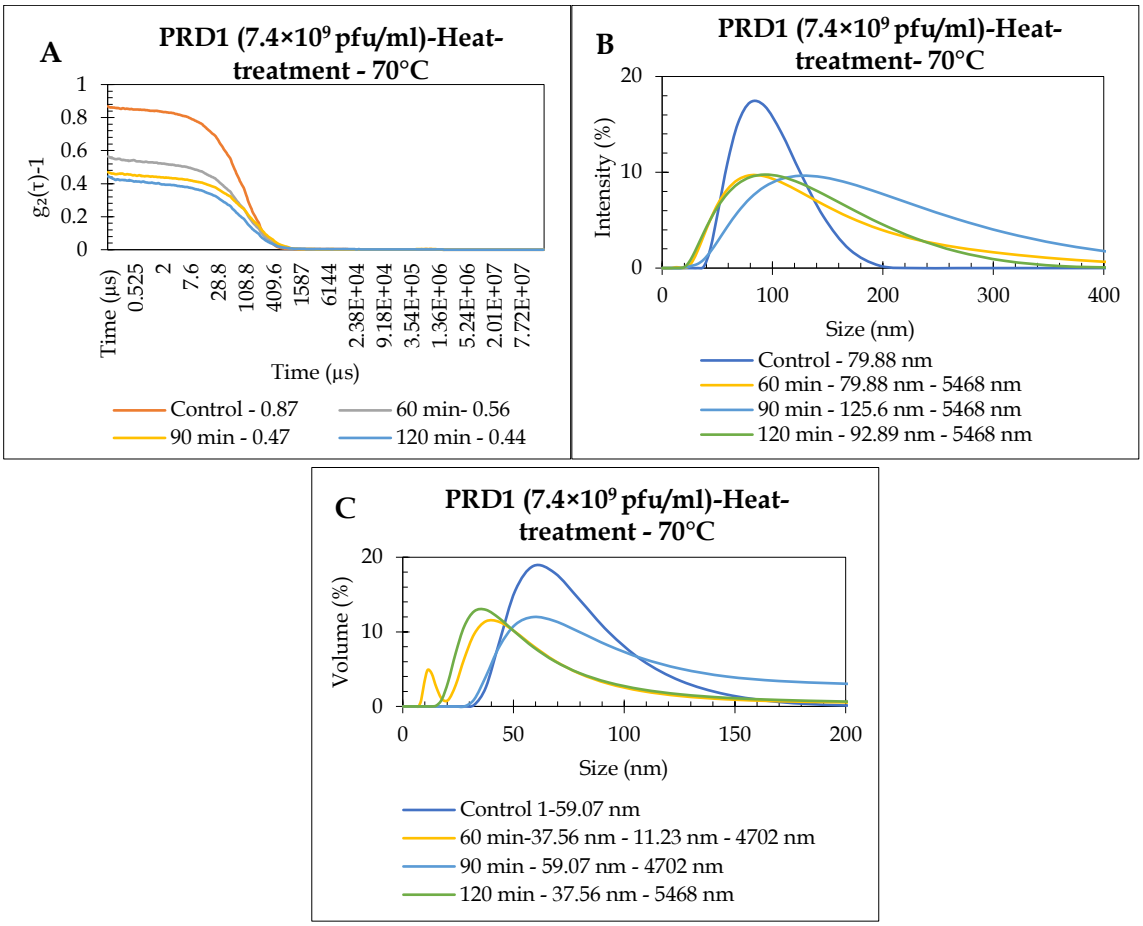

Figure 11. Heat Treatment of PRD1 Phages with initial titer of 7.4×10^{9} PFU/mL. A) Schematic illustration of the autocorrelation. B) The intensity-weighted distribution suggesting increased polydispersity. C) In the volume-weighted distribution indicating increased polydispersity after heating.

3.4.4. Sonication Induces Fragmentation and Aggregation of PRD1 Phage with Reduced Infectivity

Seven samples of PRD1 were prepared at a concentration of 10^{9} PFU/mL and sonicated for 10, 20, 30, 40, 50, or 60 seconds. A control sample with the same titer was kept at 4°C in the cold room without sonication. After sonication, the size

distribution and particle concentration of both the control and treated samples were immediately measured using DLS. The autocorrelation curves for the control and treated samples, sonicated for 10, 20, 30, 40, 50, and 60 seconds, showed intercepts of 0.85, 2.22, 4.73, 3.53, 3.66, 3.73, and 2.82, respectively (Figure 12.A). Since the intercept of control was higher than 0.6 and close to 1, it was considered a high-quality measurement. However, the intercepts of the treated samples were higher than 2, making the size measurement results unreliable.

The intensity-weighted distribution of the treated samples showed a significant difference compared to that of the control sample. The control sample had a peak at 79.88 nm, representing the hydrodynamic size of the intact phage particles, with an intensity percentage of 14.93. However, in the sample sonicated for 10 seconds, the phage peak was absent, and two sharper peaks appeared: one at 50.79 nm with an intensity percentage of 40.1, and the other at 32.3 nm with an intensity percentage of 17.74 (Figure 12.B). Although size measurement in the treated samples is not precise due to polydispersity, this distribution chart generally suggests particle fragmentation and an increase in the number of particles. The particle concentration results support this hypothesis. In the control sample, the particle concentration was 2.40×10^{9} particles/ml, but after 10 seconds of sonication, it increased to 6.28×10^{10} particles/ml.

The same trend was observed in the samples sonicated for 20, 30, 40, and 50 seconds. In addition to the disappearance of the intact PRD1 phage peak, two new peaks appeared at 37.56 nm and 9.65 nm (20 seconds), 43.68 nm and 59.07 nm (30 and 40 seconds), and 32.3 nm and 50.79 nm (50 seconds). These new peaks, with hydrodynamic sizes smaller than the complete phage, had intensity percentages significantly higher than the phage peak. This suggests the hypothesis of phage fragmentation and an increase in particle concentration. Given that particle concentration continued to increase with sonication time from 10 to 20, 30, 40, and 50 seconds, this further supports the hypothesis that particle fragmentation has occurred.

In the sample sonicated for 60 seconds, a peak was observed at 108 nm with an intensity percentage of 38.88. This peak is larger than the complete phage particles and is sharper than the phage peak, with a significantly higher intensity percentage. These results suggest particle aggregation in the sample sonicated for 60 seconds. Given that the measured particle concentration at 60 seconds is ten times less than at 50 seconds, the hypothesis of aggregation is further supported. The volume-weighted distribution chart shows a similar trend. The control peak is broader than the sonicated samples. After 10, 20, 30, 40, and 50 seconds of sonication, two much sharper peaks appeared compared to the control sample. In the sample sonicated for 60 seconds, a broader peak appeared with a size larger than the complete phage particles (Figure 12.C).

Plaque assays showed that the 10-second sonicated sample did not have a reduced titer compared to the control. The 20-second sonicated sample had a tenfold reduction in titer, while the 30, 40, 50, and 60-second sonicated samples had zero titer, indicating complete loss of viability. Thus, DLS did not assist in determining the viability of the phages (Table 9).

Table 9. DLS measurements of sonication treated of PRD1 phage samples.

Sample	Z-Average (nm)	PDI	Intercept	Peak 1 (nm)	Particle concentration (particles/ml)	Phage titer (pfu/ml)
Control	84.85	0.1368	0.84	92.89	2.40×10^{9}	3.8×10^{9}
10 sec	1621	0.9315	2.22	25.19	6.28×10^{10}	5.95×10^{9}
20sec	8763	0.8514	4.72	9.65	1.78×10^{11}	4.1×10^{8}
30 sec	3003	1	3.51	43.68	1.30×10^{11}	0
40 sec	3226	1	3.72	27.21	2.47×10^{11}	0
50 sec	3939	1	3.73	25.19	3.35×10^{11}	0
60 sec	2661	1	2.81	108	3.32×10^{10}	0

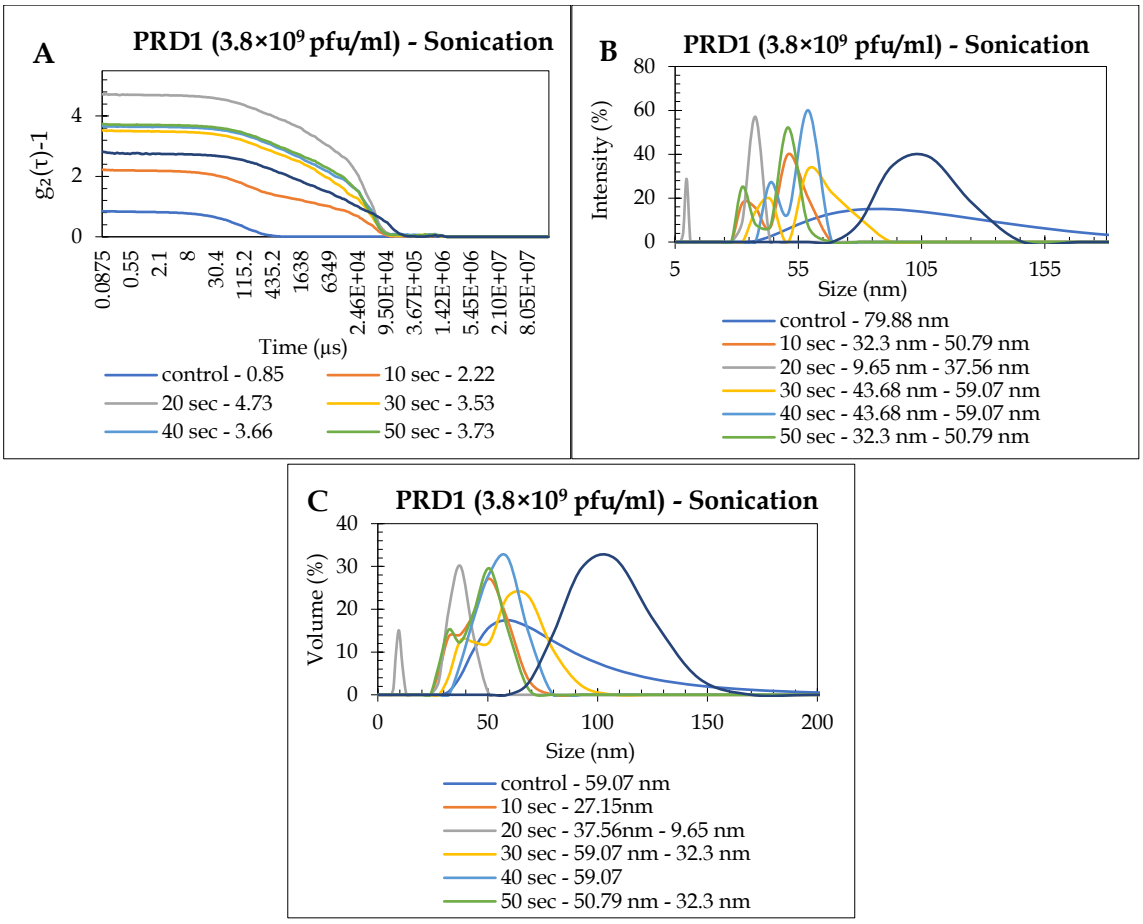

Figure 12. Sonication of PRD1 preparation with initial titer of 3.8×10^{9} PFU/mL. A) The DLS autocorrelation function (ACF) curves. B) intensity-weighted size distribution. C) volume-weighted distribution.

3.5. DLS Fails to Distinguish PRD1 and T4 in Mixed Samples

Next, the suitability of DLS method to distinguish phages with different morphologies (tailed and non-tailed) in a mixture was assessed. A 1:1 phage mixture was created using 500 µl of PRD1 phage at 3.8×10^9 PFU/mL and 500 µl of T4 phage at 1.5×10^9 PFU/mL. After vortexing, the hydrodynamic size was measured using DLS. DLS could not distinguish between the two different phages. The intensity-weighted distribution showed the mode peak at 146.1 nm which represents the size of the intact T4 phage particles (Figure 13.B).

For the next measurement, the phage titer of the T4 phage was reduced to 6.2×10^7 PFU/mL. Then, 500 µl of PRD1 at 3.8×10^9 PFU/mL was mixed with 500 µl of T4 at 6.2×10^7 PFU/mL. After changing the mixture ratio, only one peak at the size of intact PRD1 phage particles, 92.89 nm, appeared. Both measurements displayed "good" correlation functions (Figure 13.A).

The mode peak for the control PRD1 sample was 92 nm, which was larger than the hydrodynamic size of the PRD1 phage. The control sample was diluted in a buffer two weeks before the experiment. During this time, some aggregation likely occurred in the cold room. Since the intensity-weighted distribution is highly sensitive to larger particles, the mode peak was positioned higher than the hydrodynamic size of the page.

Table 10. DLS measurements of phage mixture

Sample	Z-average (nm)	PDI	Intercept	Peak 1 (nm)	Particle concentration (particles/ml)	Phage titer (pfu/ml)
Control- PRD1- 3.8×10^9	84.85	0.14	0.93	79.88	2.40×10^9	3.8×10^9
Control-T4-1.5×10^9 PFU/mL	156	0.25	0.87	146.1	1.11×10^8	6.2×10^7
500ul PRD1 3.8×10^9+500ul T4 1.5×10^9	1621	0.93	0.85	146.1	6.28×10^{10}	5.95×10^9
2500 ul PRD1 3.8×10^9+500ul T4 1.5×10^9 PFU/mL	8763	0.85	0.85	92.89	1.78×10^{11}	4.1×10^8

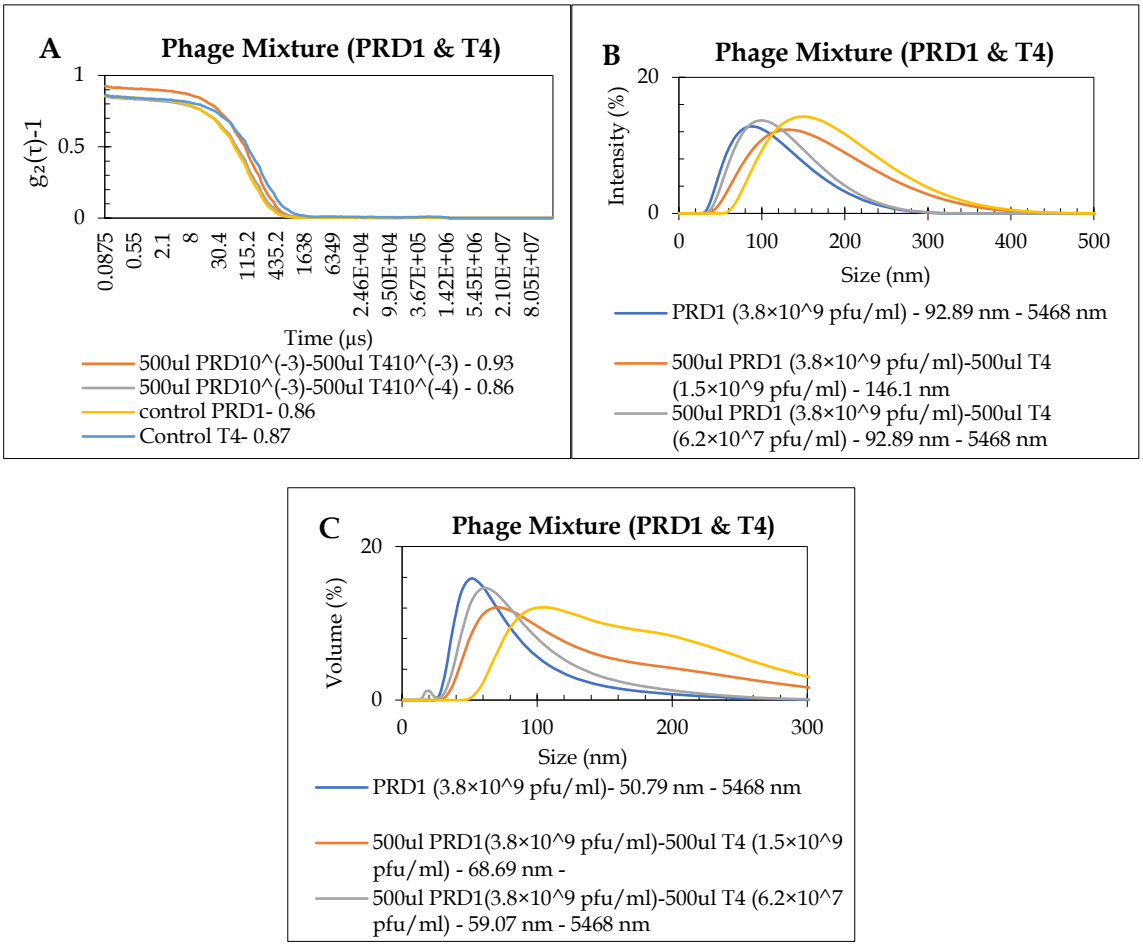

Figure 13. DLS Measurements of Phage Mixture. A) The DLS autocorrelation function ACF) curves. B) intensity-weighted size distribution. C) volume-weighted distribution.

4. DISCUSSION

At the outset, this study aimed to evaluate the effectiveness of the DLS method in assessing the physical state of phages. We report that DLS tracking of phage size distributions is an effective way to predict the aggregation and integrity of phage preparations. To achieve optimal concentration, the phages were purified through a traditional method: PEG precipitation followed by ultracentrifugation. This process resulted in the formation of two bands. Despite the enrichment of complete phage particles in the lower band, many infective phages were also present in the upper (low-density) band (Figure 2) (Appendix 3).

Previous studies have noted that combining PEG precipitation with sucrose density centrifugation provides a robust method for purifying large macromolecular complexes, serving as an orthogonal approach to PEG precipitation (Henneberg and Chari 2021). Bacteriophages can be easily concentrated from crude lysates of infected bacteria by adding PEG. Specifically, T4 bacteriophages are efficiently removed from the solution by simple settling when the concentration of PEG 6000 is between 2% and 10% (Yamamoto et al. 1970).

Some protocols use additional NaCl to enhance precipitation. The suggested mechanism of phage precipitation using PEG is very similar to the salting-out process used in protein precipitation (Atha and Ingham 1981) (Arakawa and Timasheff 1984). Bacteriophage particles are primarily composed of coat proteins surrounding their genetic material. In solutions containing PEG and high salt content, water molecules are separated, causing the bacteriophages to aggregate into clusters. Adding salts, such as NaCl, to PEG can replace some water molecules interacting with the charged coat proteins of the phage, reducing the number of available water molecules and promoting better aggregation and precipitation of the phage. Additionally, NaCl helps separate membrane-bound phages from the bacterial membrane. As a result, the precipitated phages can be easily collected by centrifugation (Archer and Liu 2009). Based on these studies, we used 10% weight/volume PEG 6000 and 0.5 M NaCl. The mixture was gently stirred for 15 minutes at 4 °C until a clear solution was achieved.

4.1. Optimal Protein Concentration for DLS Measurement

The lowest required sample concentration in DLS experiments is determined by various instrumental and sample parameters. Most DLS instruments need a minimum concentration of around 0.5 mg/mL (NanoTemper Technologies 2023). Concentrations ranging from 1 to 10 mg/mL are often a reasonable starting point for determining the appropriate sample concentration (JKweb, Webdesign Basel & Zürich).

The Bradford assay measures the total protein concentration in the sample, which includes proteins from phage particles as well as any other proteins present in the buffer. Although the Bradford assay does not provide a direct measure of phage concentration, the protein concentration obtained can be used as an indirect indicator. This indirect measure can help determine if the protein concentration is within a suitable range for DLS analysis, thus aiding in the estimation of whether the sample concentration is appropriate for accurate measurement.

The concentration of our phage samples was lower than the range recommended by previous studies for DLS measurements (Figure 3). The T4 phage had a titer of 2.4×10^{8} PFU/mL and a protein concentration of 0.027 µg/µl (Table 3). The PRD1 phage had a titer of 7.8×10^{11} PFU/mL yielding a protein concentration of 0.021 µg/µl (Table 7). These protein concentrations were deemed appropriate for our DLS measurement experiments.

4.2. Hydrodynamic size of the T4 and PRD1 phages

We determined the hydrodynamic size of the T4 phage using DLS and obtained a measurement of 146.1 nm (Table 3). This size closely aligns with the average diameter of the T4 phage reported in previous studies: 137.9 ± 1.06 nm, with a narrow size distribution and a PDI of 0.030 ± 0.023 (Szermer-Olearnik et al., 2017).

DLS interprets results using a spherical model, assuming particles exhibit spherical behavior. However, T4 phages do not entirely fit this model, and their measurements are interpreted as if they were spherical (Szermer-Olearnik et al. 2017). Therefore, the hydrodynamic size of T4 is different from its actual size, as seen under high-resolution electron microscopy (Willey et al. 2008).

We measured the hydrodynamic size of PRD1 at 78.4 nm, which aligns with the sizes reported in other studies (Table 7). In a study by Mesquita et al., the size of PRD1 was measured using both DLS and SEM. The SEM results showed a cubic (icosahedral) capsid with no tail, measuring 63 nm, while the DLS measurements indicated a size of 82 ± 6 nm (Mesquita et al. 2010).

In our study, the discrepancy between the hydrodynamic size and the actual size of T4 was 53.9 nm, which is greater than the 15.4 nm size difference observed for PRD1. This is because PRD1 has an icosahedral capsid and therefore fits better in the DLS model, while phage T4 has a more elongated structure and a tail.

4.3. Cumulants analysis (z-average, and PDI)

The Polydispersity Index (PDI) is a dimensionless measure that ranges from 0 for monodisperse samples to 1 for polydisperse samples. In practice, the best values for monodisperse samples are around 0.05. PDI values below 0.05 are typically observed with latex standards or particle dispersions. DLS can only provide a monomodal (single peak) distribution within this range. From 0.08 to 0.7, the mid-range PDI values represent the range where distribution algorithms perform most effectively. PDI values above 0.7 indicate a very broad particle size distribution (Tosi et al. 2020).

The z-average diameter is the intensity-weighted mean diameter derived from cumulant analysis. Cumulant analysis, while providing z-average and PDI, has its limitations. A primary limitation of cumulant analysis is that it only describes a single average-size result using the z-average value. This method cannot identify individual modes in populations that deviate significantly from a monomodal distribution. As a population's modality increases, the effectiveness of cumulant analysis in providing useful information decreases (Tosi et al. 2020).

In the study by Szermer-Olearnik et al., reducing the ionic strength to 10 mM significantly altered the distribution of T4 particles. The autocorrelation curve in a low ionic strength environment indicated a rapid increase in the presence of larger aggregates. The z-average increased approximately with the square root of time, suggesting a diffusion-regulated aggregation process. This behavior underscores the impact of ionic strength on particle dynamics and aggregation in solution. In the

same study it is mentioned that in the polydisperse system, particle clusters varied in size and form. As a result, 'average diameter' for a given time point should not be taken as the typical measurement of aggregates (Szermer-Olearnik et al. 2017).

In our study, the untreated control samples showed high-quality measurements with intercepts between 0.6 and 1. The PDI ranged from 0.05 to 0.32, and the z-average was 150.6-180.8 nm for T4 and 78.4-84.85 nm for PRD1.

The z-average for the sonicated samples was 2866-4264 nm for T4 and 1621-8763 nm for PRD1 (Table 5 and 9). For heated samples, the z-average was 177.8-193.7 nm for T4 and 85-114 nm for PRD1 (Table 4 and 8). The sonicated T4 samples had intercepts greater than 1, specifically ranging from 2.76 to 4.22, with PDIs of 1. Similarly, PRD1 sonicated samples had intercepts above 2, with PDIs ranging from 0.85 to 1 and z-averages from 1621 nm to 8763 nm. Heat-treated T4 samples showed intercepts of 0.5, PDIs of 0.30, 0.26, and 0.24, and z-averages of 193.7 nm, 181.9 nm, and 177.8 nm. Heated PRD1 samples had intercepts lower than 0.4, PDIs of 0.34, 0.29, and 0.26, and z-averages of 85 nm, 114 nm, and 85 nm. These results suggest that due to high polydispersity and sample aggregation, the size distribution for sonicated and heat-treated samples is not reliable.

Our study demonstrates that DLS Cumulants analysis provides valuable insights into the physical state of phages despite some inherent limitations. For untreated control samples, the analysis indicated uniform particle size distributions with intercepts between 0.6 and 1. The z-average in homogenous monodisperse phage samples represents the hydrodynamic size of intact phage particles.

When sonicated and heated samples were compared to control samples, there were significant changes in the intercept values and z-average. Sonicated T4 samples had intercepts greater than one and z-averages ranging from 2866 nm to 4264 nm, and sonicated PRD1 samples had intercepts greater than two and z-averages ranging from 1621 nm to 8763 nm. The increase in z-average likely indicates aggregation. However, due to the high polydispersity of these samples, the data quality is low, making it difficult to determine the precise hydrodynamic size of the aggregates. Similarly, heat-treated T4 and PRD1 samples showed intercepts lower than 0.6, indicating unreliable measurements. Despite this, the deviations still suggest significant changes in the physical state of the particles.

Our research showed that DLS cumulant analysis works very well for homogeneous, uniform samples, giving accurate readings that show how the particles are distributed in size. However, particle size characterization becomes challenging for samples with high polydispersity, such as those undergoing physical stress, while the analysis can detect physical changes. Thus, it should be complemented by other analytical methods to ensure comprehensive and accurate characterization.

4.4. Distribution analysis (distribution of sizes)

Studies have demonstrated that many environmental factors and handling procedures can cause phage damage and titer loss, with aggregation being a common consequence. Researchers have reported using DLS to track phage size

distributions, finding it to be an effective method for predicting the bioactivity of phage preparations in a semi-quantitative to quantitative manner ("Correction to: Rapid assessment of changes in phage bioactivity using dynamic light scattering" 2024b).

Particle size distributions can be plotted in three ways: by intensity, volume, or number of particles. Volume and number size distributions are derived from the primary intensity-weighted distribution using Mie Theory. Since the DLS technique relies on changes in light intensity due to Rayleigh scattering, the primary size distribution obtained from a DLS measurement is the intensity-weighted distribution. The intensity-weighted distribution is highly sensitive to the presence of large particles or aggregates. For example, if we analyze a sample containing an equal number of particles of 100 nm and 10 nm in diameter, the DLS results will show a distribution with two peaks. The peak corresponding to the larger particles will have an area 10^6 times greater than that of the peak for the smaller particles. Therefore, the intensity-weighted distribution does not accurately reflect the actual number of particles in polydisperse samples.

The volume-weighted size distribution is also sensitive to large particles. However, converting the intensity-weighted distribution into volume-weighted distributions provides a more realistic representation of the sample composition. For the volume-weighted distribution, the peak for the larger particles will be 10^3 times higher than that of the same number of smaller particles. However, the volume-weighted distribution should only be used to estimate the relative amounts of material in distinct peaks since the means and particularly the widths are less reliable. For reporting the size of each peak in the distribution, it is more accurate to use the primary intensity-weighted size distributions (Tosi et al. 2020).

In our study, the size distribution based on intensity for untreated, monodispersed phage samples showed the most accurate hydrodynamic size for the phages. Therefore, we reported the hydrodynamic size of phages T4 and PRD1 based on the intensity-weighted distribution (Figure 9 and 4). In a homogenous monodisperse sample without contamination and impurities, we expect only a single sharp Gaussian peak, which should represent the size of the complete phage particles. In some control samples, a peak around 5460 nanometers is also observed, which may be due to aggregation during storage of the phage at 4°C. This impurity can negatively affect the reliability of the intensity-weighted distribution of the purified sample. Therefore, it is recommended that in future experiments, the tests be conducted immediately after phage purification to minimize the impact of impurities on the validity of the results.

In polydisperse samples, the volume-weighted distribution provides a more realistic depiction of the sample. For instance, in heat-treated T4 samples, the difference between the control and heat-treated samples is not very clear in the intensity-weighted distribution. However, in the volume-weighted distribution, all heat-treated samples show a significant difference compared to the control. From 90 to 130 degrees, the volume percentage is almost halved, and distinct peaks are observed. The 60-degree heat-treated sample shows that the size of peak1 is almost double that of the peak1 of the control sample. Therefore, the effect of heat, which

increased polydispersity, was very clearly visible in the volume-weighted distribution.

The same results apply to PRD1 as well. However, for phage PRD1, the difference between volume and intensity-weighted distribution is less compared to phage T4. For phage PRD1, the heat-treated samples have almost half the volume and intensity percentage of the control peak, and the peaks after heat treatment are nearly twice as broad. The volume-weighted distribution again provides a clearer representation of the size distribution, with distinct peaks observed for the 60-minute heat-treated sample.

The difference between the size distribution of control and sonicated samples for both phages is much greater than that of heat-treated samples because sonication has a more significant effect on increasing polydispersity. For instance, in the case of sonicated T4 phage samples, both intensity and volume-weighted size distributions show that the control sample has a single peak around the hydrodynamic size of the intact phage. However, the sonicated samples exhibit several distinct, sharp peaks with intensity or volume percentages nearly more than double that of the control phage.

Very similar results were observed for PRD1 phage. The control phage only displays a single peak around the size of the intact phage, whereas the sonicated samples show multiple distinct, sharp peaks with higher volume or intensity percentages than those of the control peak. Additionally, the 60-second sonicated sample shows a very different peak at a size larger than that of the control sample.

The distribution charts were unable to distinguish between PRD1 and T4 phages, showing only a single peak for the sample containing a mix of phages. The main reason is that the hydrodynamic sizes of the T4 and PRD1 phages differ by approximately 70 nanometers. Thus, the device cannot detect two distinct peaks and instead displays these two phages as a broad single peak.

Additionally, it should be noted that the PRD1 phage sample had been stored in a cold room for several weeks, causing its size to increase from 78 nanometers to 92.89 nanometers. This aggregation also contributed to the merging of the peaks. If the size difference between the phages were greater, the intensity and volume-weighted size distribution would likely be able to indicate the presence of different phages.

4.5. Autocorrelation function

Autocorrelation function curves are essential for characterizing particle size changes in solutions, as smaller particles exhibit shorter correlation times compared to larger ones. Carvalho et al. (2014) demonstrated that denaturation and aggregation can be monitored through autocorrelation curves. At 60 and 65 °C, the autocorrelation curves displayed oscillations, indicating non-diffusive properties or very high-count rates, which align with the presence of large aggregates in the solution. This study highlights the utility of autocorrelation analysis in

understanding particle dynamics and stability under varying conditions (Carvalho et al. 2014).

Misono (2019) describes that Oscillations in the autocorrelation curve in DLS suggest complicated dynamics within the sample, such as a polydisperse particle size distribution. These oscillations can also be caused by multiple scattering events, high particle concentrations that cause interactions, or structural rearrangements in complex fluids. This understanding is critical for interpreting DLS data and properly defining particle behaviors under different situations (Misono 2019).

The intercept value can be used to evaluate the signal-to-noise ratio from a measured sample and thus is often used to judge data quality. It is usually scaled such that an ideal signal will give a value of 1, and a good system will give intercepts more than 0.6, and greater than 0.9 for the best systems ('Dynamic Light Scattering (DLS) - Definition & Terms | Malvern Panalytical'). A lower-than-expected value may indicate too high or too low a sample concentration, absorption or fluorescence of the sample. Too high a sample concentration may lead to multiple scattering effects that will reduce the intercept value.

In our study, both heating and sonication have significantly affected the intercept values of the samples. Heating generally decreases the intercept values, as seen in both T4 and PRD1 heated samples, which have lower intercept ranges (0.50 to 0.57 for T4 and 0.43 to 0.56 for PRD1) compared to their control and L-Pellet counterparts. Sonication, on the other hand, dramatically increases the intercept values, as observed in the sonicated T4 samples (2.76 to 4.22) and sonicated PRD1 samples (2.22 to 4.72). Therefore, heating tends to decrease the intercept values, indicating a possible reduction in particle size or aggregation, while sonication increases the intercept values, suggesting an increase in particle size distribution or polydispersity.

4.6. Comparing DLS and plaque assay results

To determine if DLS can detect the biological activity of phages, we performed plaque assays for most of the samples measured by DLS. Due to time constraints, plaque assay results were missing for some samples. However, we made an effort to gather sufficient data from both untreated and treated samples to enable a realistic evaluation of DLS's capability to measure the biological activity of phages.

The data shows a strong correlation between the titer and the particle concentration of the untreated purified T4 phage samples. The samples with titers of 1.5×10^9, 2.4×10^8, and 1.8×10^7 PFU/mL, had particle concentrations of 4.89×10^9, 7.12×10^8, and 5.56×10^7 paticles/ml. This indicates that as the titer of the phage decreases, the particle concentration measured by DLS also decreases proportionally. The peak1 for all three samples represents the size of the complete T4 phage particles, suggesting that the majority of the particles counted are intact phage particles. The strong correlation between phage titer and particle concentration indicates that the DLS is reliable for assessing the bioactivity of monodispersed and purified phage samples.

In the T4 sonication experiment, the control sample containing untreated phage had again nearly identical particle concentration and phage titer, with a phage titer of 1.26×10^8 PFU/mL and a particle concentration of 2.31×10^8 paticles/ml. However, after sonication under two different programs, particle concentrations increased to 2.23×10^9 and 1.54×10^9 paticles/ml, while phage titers decreased to 5.6×10^7 and 1.5×10^7 PFU/mL, respectively. This indicates that in the treated samples, a portion of the phages were damaged, leading to a tenfold decrease in phage titer and a tenfold increase in particle concentration. This suggests that the inactivation of some phages may be due to fragmentation and loss of phage integrity under mechanical stress. Additionally, changes in size distribution for sonicated phages and appearing several distinct peaks confirm this damage. Therefore, while DLS results could not directly measure the reduction in phage bioactivity, they clearly indicated physical alterations in the phages, suggesting a likely decrease in bioactivity.

The results for phage PRD1 differed slightly from expectations. We anticipated a tenfold decrease in phage titer with a tenfold increase in phage dilution. However, with a hundredfold increase in the dilution of purified phage PRD1, the phage titer decreased from 8×10^{12} to 4.3×10^{11}, showing only a tenfold reduction. Additionally, the difference between the 100-fold diluted phage and the 1000-fold diluted sample was less than expected. This could be due to the small size of the phage. The small size of phage PRD1 could contribute to its behavior during dilution. Smaller particles might be more prone to interactions with container surfaces or might diffuse differently, impacting the effective concentration in the solution. Phages might also form aggregates or clusters. At higher concentrations, these clusters could remain intact, but as the solution is diluted, these clusters might not disperse completely, leading to fewer effective phage particles than expected.

The relationship between phage titer and particle concentration for PRD1 was slightly different from that for phage T4. The phage titer for the serially diluted purified phage PRD1 samples was 4.3×10^{11}, 7.8×10^{11}, and 4.7×10^{10} PFU/mL, while the particle concentrations for these samples were 2.35×10^{10}, 1.42×10^{10}, and 1.69×10^9 paticles/ml, respectively. In fact, for each sample, the particle concentration was ten times lower than the phage titer, unlike phage T4, where the particle concentration was almost equal to the phage titer. Again, this could be because PRD1 might have a higher tendency to form aggregates or clusters that are not fully separated during dilution or measurement. These aggregates can lead to an underestimation of the titer, as multiple infective phages within an aggregate might be counted as a single particle.

This error in the heating experiment of phage PRD1 was somehow corrected. The 1000-fold diluted phage sample (control) had a titer of 7.4×10^9 PFU/mL as we expected, and its particle concentration measured by DLS was almost equal to the phage titer, at 8.53×10^9 PFU/mL. After 60, 90, and 120 minutes of heating, the phage titer decreased to 7.15×10^6, 7.4×10^6, and 5.5×10^6 PFU/mL, respectively, showing an almost 1000-fold reduction, indicating that some phages lost their biological activity during the heating process. The particle concentrations for the heated samples were 1.54×10^{10}, 5×10^8, and 2.45×10^8 paticles/ml, respectively. In the 60-minute heated

sample, the particle concentration increased tenfold, while in the 90 and 120-minute samples, it decreased tenfold. These results, along with the distribution chart, suggest that at lower temperatures, some particles fragmented, and at higher temperatures, aggregation occurred, explaining the changes in particle concentration. In any case, both the fragmented and aggregated particles likely lost their infectivity since a similar reduction in phage titer was observed in all three samples.

Therefore, similar to the phage T4 sample, observing changes in particle concentration and size distribution suggests that part of the phage sample has lost its biological activity. However, accurately predicting the type and extent of damage using DLS was not possible.

In the phage sonication experiment, the control sample showed nearly identical predicted particle concentration and phage titer. After twenty seconds of sonication, the particle concentration increased tenfold, while the phage titer remained unchanged. After thirty seconds of sonication, the particle concentration increased almost a hundredfold, and the titer decreased by approximately ten times. Data on the phage titer for samples sonicated for longer durations is not available.

If the phage sample is monodispersed and free from contamination, as observed in all control samples, the particle concentration measured by DLS will closely match the phage titer. The mode peak for the intensity-weighted distribution of the control samples will be Gaussian. However, after treatment and subsequent damage to the phages, changes in particle concentration, size distribution, or both will be observable. These changes allow us to predict a reduction in titer using DLS, although accurately quantifying the reduction or determining the type of damage was not possible in our experiment.

The study by Dharmaraj et al. (2023) compared plaque assays and DLS for assessing phages, focusing on titer loss and size alterations. Plaque assays measure the infectivity of phages by counting plaques formed on a bacterial lawn, crucial for applications like phage therapy. DLS assesses the size distribution and aggregation state of phage particles, providing insights into their physical stability. The results indicated that while both methods are valuable, they serve complementary purposes: plaque assays evaluate phage infectivity, whereas DLS offers information on physical stability and aggregation.

Szermer-Olearnik et al. (2017) demonstrated that DLS predictions of phage titer loss is accurate and that DLS can provide clinically relevant information on the activity of a phage sample prior to its use. They have shown that DLS tracking of phage size distributions is a valuable tool for forecasting the bioactivity of phage preparations in a semi-quantitative to quantitative manner. Once standard curves are established to correlate changes in physical condition with bioactivity, DLS proves to be quicker, more efficient, and less damaging than plaque assays. However, the study also acknowledges the limitations of DLS in fully assessing the bioactivity of phages (Szermer-Olearnik et al. 2017).

Some studies suggest that aggregation can be a mechanism for increasing phage survival at mild temperatures. Bożena et al. (Szermer-Olearnik et al. 2017) showed that phages in aggregates were more resistant to extreme environmental

conditions like heat. However, we still need to directly address or propose the possibility of aggregation as a mechanism for increasing phage survival at mild temperatures.

5. CONCLUSION

DLS is an effective technique to analyze the physical properties of phages, including the hydrodynamic size and aggregation state. DLS measures the hydrodynamic diameter of the T4 phage to be 146.1 nm and the PRD1 phage to be 79.88 nm. Additionally, DLS is effective in detecting changes in phage size distributions that result from treatments such as heat and sonication.

The combined results from DLS and plaque assays show that heat treatment significantly disrupts phage integrity and infectivity. For both PRD1 and T4 phages, heating leads to increased polydispersity, aggregation, fragmentation, and a reduction in particle concentration and phage titer. Similarly, sonication causes substantial changes, with both phages exhibiting higher z-averages (above 1500 nm) and increased intercept values (greater than 2), indicating notable structural alterations. Sonication results in fragmentation, an increase in particle concentration, and a reduction in titer.

When assessing size distributions, the volume-weighted distribution method is preferable for polydisperse samples, such as those subjected to heat or sonication, because it provides a more accurate representation by minimizing the influence of larger particles. In contrast, for homogeneous and monodisperse samples, the intensity-weighted distribution method is more suitable, as it offers clearer and more precise measurements.

Despite its strengths, DLS has limitations, especially in distinguishing between different phage types in mixtures. For example, in a 1:1 mixture of T4 and PRD1 phages, the DLS signal was dominated by the larger T4 particles, which obscured the presence of the smaller PRD1 particles. Therefore, while DLS is effective for measuring phage size in monodisperse samples and detecting physical changes, it should be used alongside other methods, such as plaque assays, to fully evaluate the impact of stress factors on phage structure and functionality.

6. ACKNOWLEDGEMENTS

The research presented in this thesis was conducted within the group led by Lotta-Riina Sundberg at the University of Jyväskylä, from December 2023 to March 2024. This period has been both enriching and transformative, and I extend my sincere gratitude to all who have supported me throughout this journey.

First and foremost, I express my deepest gratitude to my supervisors, Lotta-Riina Sundberg, Elina Laanto, and Kaisa Helttunen, for providing me with this remarkable opportunity. Their invaluable guidance, expertise, and unwavering support were instrumental in shaping this research and helping me navigate the challenges encountered during this project.

I am also profoundly grateful to Janne Ihalainen, my master's program supervisor, for his indispensable advice and mentorship over the past two years. His insights and suggestions have significantly contributed to my academic growth.

Special thanks are due to Leena Mattila for her invaluable assistance in managing my schedule, which greatly contributed to my ability to balance academic responsibilities effectively. I am also grateful to Tarja Aalto for her unwavering encouragement and support throughout this period. To all those who have played a pivotal role in my academic journey, I extend my deepest gratitude. I owe my current position and accomplishments to their guidance and support.

Jyväskylä, August 2024
Hanieh Shirvani

7. REFRENCES

1. Goodridge L.D. & Abedon S. 2002. Bacteriophage biocontrol and bioprocessing: Application of phage therapy to industry. *SIM News* 53.
2. Drulis-Kawa Z., Majkowska-Skrobek G. & Maciejewska B. 2015. Bacteriophages and Phage-Derived Proteins – Application Approaches. *Current Medicinal Chemistry* 22: 1757–1773.
3. Inal J.M. 2003. Phage therapy: a reappraisal of bacteriophages as antibiotics. *Archivum Immunologiae Et Therapiae Experimentalis* 51: 237–244.
4. Jiang S.C. & Paul J.H. 1998. Significance of Lysogeny in the Marine Environment: Studies with Isolates and a Model of Lysogenic Phage Production. *Microbial Ecology* 35: 235–243.
5. Zalewska-Piątek B. 2023. Phage Therapy—Challenges, Opportunities and Future Prospects. *Pharmaceuticals* 16: 1638.
6. Rahimi-Midani A., Lee S.-W. & Choi T.-J. 2021. Potential Solutions Using Bacteriophages against Antimicrobial Resistant Bacteria. *Antibiotics* 10: 1496.
7. Eaves E. 2018. Bacteriophages: a promising approach to fighting antibiotic-resistant bacteria. *Bulletin of the Atomic Scientists*.
8. Twort F.W. 1915. AN INVESTIGATION ON THE NATURE OF ULTRA-MICROSCOPIC VIRUSES. *The Lancet* 186: 1241–1243.
9. d'Hérelle F. Sur un microbe invisible antagoniste des bacilles dysentérique. *Acad Sci Paris.* 1917;165:373–5
10. Sulakvelidze A., Alavidze Z. & Morris J.G. 2001. Bacteriophage Therapy. *Antimicrobial Agents and Chemotherapy* 45: 649–659.
11. Royer S., Morais A.P. & Da Fonseca Batistão D.W. 2021. Phage therapy as strategy to face post-antibiotic era: a guide to beginners and experts. *Archives of Microbiology* 203: 1271–1279.
12. Karuppannan S, Kumar K, Vo TTN, Jeong KY. 2024. Recent advances in biomaterial-based wound healing therapies: A narrative review. *Journal of Advanced Research*. 48:197-220. doi:10.1016/j.jare.2023.05.006.
13. Daubie V., Chalhoub H., Blasdel B., Dahma H., Merabishvili M., Glonti T., De Vos N., Quintens J., Pirnay J.-P., Hallin M. & Vandenberg O. 2022. Determination of phage susceptibility as a clinical diagnostic tool: A routine perspective. *Frontiers in Cellular and Infection Microbiology* 12: 1000721.
14. Abedon S.T. 2018. Detection of Bacteriophages: Phage Plaques. In: Harper D.R., Abedon S.T., Burrowes B.H. & McConville M.L. (eds.), *Bacteriophages: Biology, Technology, Therapy*, Springer International Publishing, Cham, pp. 1–32.
15. Ramesh N., Archana L., Royam M.M., Manohar P. & Eniyan K. 2019. Effect of various bacteriological media on the plaque morphology of Staphylococcus and Vibrio phages. *Access Microbiology* 1.
16. Toister E., Cherry L., Lupu E., Monash A., Dor E., Levin L., Girshengorn M., Natan N., Chapman S., Shmaya S., Epstein E., Adar Y., Zichel R., Ophir Y. &

Diamant E. 2024. Development and Validation of a Plaque Assay to Determine the Titer of a Recombinant Live-Attenuated Viral Vaccine for SARS-CoV-2. *Vaccines* 12: 374.
17. Han C. & Yang C. 2014. Viral Plaque Analysis on a Wide Field-of-view, Time-lapse, On-chip Imaging Platform. *The Analyst* 139: 3727–3734.
18. Abedon S.T. & Katsaounis T.I. 2019. Detection of Bacteriophages: Statistical Aspects of Plaque Assay. In: Harper D.R., Abedon S.T., Burrowes B.H. & McConville M.L. (eds.), *Bacteriophages: Biology, Technology, Therapy*, Springer International Publishing, Cham, pp. 1–23.
19. Tan Z.H. 2014. Biosorption of Heavy Metals onto the Surface of Bacteriophage T4. *School of Biological Sciences: Dissertations, Theses, and Student Research*.
20. Marton H.L., Kilbride P., Ahmad A., Sagona A.P. & Gibson M.I. 2023. Anionic Synthetic Polymers Prevent Bacteriophage Infection. *Journal of the American Chemical Society* 145: 8794–8799.
21. Aminoglycoside antibiotics inhibit phage infection by blocking an early stage of the infection cycle.
22. Obořilová R., Šimečková H., Pastucha M., Klimovič Š., Víšová I., Přibyl J., Vaisocherová-Lísalová H., Pantůček R., Skládal P., Mašlaňová I. & Farka Z. 2021. Atomic force microscopy and surface plasmon resonance for real-time single-cell monitoring of bacteriophage-mediated lysis of bacteria. *Nanoscale* 13: 13538–13549.
23. Leroux B.M., Henry M., Biswas B. & Pope R.K. 2018. The Use of Scanning Electron Microscopy for the Analysis of Bacteriophage Binding to Acinetobacter baumanii. *Microscopy and Microanalysis* 24: 1310–1311.
24. Thomas S., Thomas R., Zachariah A.K. & Mishra R.K. 2017. *Thermal and Rheological Measurement Techniques for Nanomaterials Characterization*. Elsevier.
25. Haar D.T. 1969. *Quantentheorie: Einführung und Originaltexte*. De Gruyter.
26. Stetefeld J., McKenna S.A. & Patel T.R. 2016. Dynamic light scattering: a practical guide and applications in biomedical sciences. *Biophysical Reviews* 8: 409–427.
27. Dharmaraj T., Kratochvil M.J., Pourtois J.D., Chen Q., Hajfathalian M., Hargil A., Lin Y.-H., Evans Z., Oromí-Bosch A., Berry J.D., McBride R., Haddock N.L., Holman D.R., Belleghem J.D. van, Chang T.H., Barr J.J., Lavigne R., Heilshorn S.C., Blankenberg F.G. & Bollyky P.L. 2023. Rapid assessment of changes in phage bioactivity using dynamic light scattering. *bioRxiv*: 2023.07.02.547396.
28. Clement S., Gardner B., Razali W.A.W., Coleman V.A., Jämting Å.K., Catchpoole H.J., Goldys E.M., Herrmann J. & Zvyagin A. 2017. Quantification of nanoparticle concentration in colloidal suspensions by a non-destructive optical method. *Nanotechnology* 28: 475702.
29. JKweb, Webdesign Basel & Zürich. LS Instruments | Experimental Guidelines - DLS Sample Preparation.

30. Technologies N. 2023. What to consider when adding DLS to your biologics early development workflow (FAQs and practical tips). *NanoTemper Technologies*.
31. Skaradzińska A., Ochocka M., Śliwka P., Kuźmińska-Bajor M., Skaradziński G., Friese A., Roschanski N., Murugaiyan J. & Roesler U. 2020. Bacteriophage amplification – A comparison of selected methods. *Journal of Virological Methods* 282: 113856.
32. Fortier L.-C. & Moineau S. 2009. Phage Production and Maintenance of Stocks, Including Expected Stock Lifetimes. In: Clokie M.R.J. & Kropinski A.M. (eds.), *Bacteriophages*, Humana Press, Totowa, NJ, pp. 203–219.
33. Yamamoto K.R., Alberts B.M., Benzinger R., Lawhorne L. & Treiber G. 1970. Rapid bacteriophage sedimentation in the presence of polyethylene glycol and its application to large-scale virus purification. *Virology* 40: 734–744.
34. Atha D.H. & Ingham K.C. 1981. Mechanism of precipitation of proteins by polyethylene glycols. Analysis in terms of excluded volume. *Journal of Biological Chemistry* 256: 12108–12117.
35. Chan-Wha K. & Kyun Rha C. 1996. Salting-out Effect on the partition of protein in Aqueous two-phase systems. *Journal of microbiology and biotechnology* 6: 352–357.
36. Ranveer S.A., Dasriya V., Ahmad M.F., Dhillon H.S., Samtiya M., Shama E., Anand T., Dhewa T., Chaudhary V., Chaudhary P., Behare P., Ram C., Puniya D.V., Khedkar G.D., Raposo A., Han H. & Puniya A.K. 2024. Positive and negative aspects of bacteriophages and their immense role in the food chain. *npj Science of Food* 8: 1.
37. Harding S.E. & Jumel K. 1998. Light Scattering. *Current Protocols in Protein Science* 11.
38. Farrell E. & Brousseau J.-L. 2018. Guide for DLS sample Preparation. *Brookhaven Instruments*. https://www.research.colostate.edu/wp-content/uploads/2018/11/Guide_for_DLS_sample_preparation.pdf
39. Ruiz E., Orozco V.H., Hoyos L.M. & Giraldo L.F. 2022. Study of sonication parameters on PLA nanoparticles preparation by simple emulsion-evaporation solvent technique. *European Polymer Journal* 173: 111307.
40. Jończyk-Matysiak E., Łodej N., Kula D., Owczarek B., Orwat F., Międzybrodzki R., Neuberg J., Bagińska N., Weber-Dąbrowska B. & Andrzej G. 2019. Factors determining phage stability/activity: challenges in practical phage application. *Expert Review of Anti-infective Therapy* 17.
41. Pirnay J.-P., Blasdel B., Bretaudeau L., Buckling A., Chanishvili N., Clark J., Corte-Real S., Debarbieux L., Dublanchet A., De Vos D., Gabard J., García M., Goderdzishvili M., Andrzej G., Hardcastle J., Huys I., Kutter E., Lavigne R., Merabishvili M. & Van den Eede G. 2015. Quality and Safety Requirements for Sustainable Phage Therapy Products. *Pharmaceutical research* 32.
42. Vörös Z., Csík G., Herényi L. & Kellermayer M. 2018. Temperature-Dependent Nanomechanics and Topography of Bacteriophage T7. *Journal of Virology* 92: e01236-18.

43. Virus Inactivation Mechanisms: Impact of Disinfectants on Virus Function and Structural Integrity | Environmental Science & Technology.
44. Qiu X. 2012. Heat Induced Capsid Disassembly and DNA Release of Bacteriophage λ. *PloS one* 7: e39793.
45. Jespers L., Schon O., Famm K. & Winter G. 2004. Aggregation-resistant domain antibodies selected on phage by heat denaturation. *Nature Biotechnology* 22: 1161–1165.
46. Szermer-Olearnik B., Drab M., Mąkosa M., Zembala M., Barbasz J., Dąbrowska K. & Boratyński J. 2017. Aggregation/dispersion transitions of T4 phage triggered by environmental ion availability. *Journal of Nanobiotechnology* 15: 32.
47. Vörös Z., Csík G., Herényi L. & Kellermayer M. 2018. Temperature-Dependent Nanomechanics and Topography of Bacteriophage T7. *Journal of Virology* 92: e01236-18.
48. Lu N., Tian Y., Wei L., Zhang G., Xie C., He T., Xu Y., Hu Z. & Wang G. 2023. Effect of ultrasound with methylene blue as sound sensitive agent on virus inactivation. *Medicine in Novel Technology and Devices* 17: 100204.
49. Nunes B.V., Da Silva C.N., Bastos S.C. & De Souza V.R. 2022. Microbiological Inactivation by Ultrasound in Liquid Products. *Food and Bioprocess Technology* 15: 2185–2209.
50. Li W., Ma H., He R., Ren X. & Zhou C. 2021. Prospects and application of ultrasound and magnetic fields in the fermentation of rare edible fungi. *Ultrasonics Sonochemistry* 76: 105613.
51. Chrysikopoulos C.V., Manariotis I.D. & Syngouna V.I. 2013. Virus inactivation by high frequency ultrasound in combination with visible light. *Colloids and Surfaces B: Biointerfaces* 107: 174–179.
52. Ultrasound–biophysics mechanisms - ScienceDirect.
53. Filipić A., Lukežič T., Bačnik K., Ravnikar M., Ješelnik M., Košir T., Petkovšek M., Zupanc M., Dular M. & Aguirre I.G. 2022. Hydrodynamic cavitation efficiently inactivates potato virus Y in water. *Ultrasonics Sonochemistry* 82: 105898.
54. Yap M.L. & Rossmann M.G. 2014. Structure and function of bacteriophage T4. *Future Microbiology* 9: 1319–1327.
55. Bichet M.C., Chin W.H., Richards W., Lin Y.-W., Avellaneda-Franco L., Hernandez C.A., Oddo A., Chernyavskiy O., Hilsenstein V., Neild A., Li J., Voelcker N.H., Patwa R. & Barr J.J. 2021. Bacteriophage uptake by mammalian cell layers represents a potential sink that may impact phage therapy. *iScience* 24: 102287.
56. Fokine A., Chipman P.R., Leiman P.G., Mesyanzhinov V.V., Rao V.B. & Rossmann M.G. 2004. Molecular architecture of the prolate head of bacteriophage T4. *Proceedings of the National Academy of Sciences of the United States of America* 101: 6003–6008.
57. Sathaliyawala T., Rao M., Maclean D.M., Birx D.L., Alving C.R. & Rao V.B. 2006. Assembly of Human Immunodeficiency Virus (HIV) Antigens on

Bacteriophage T4: a Novel In Vitro Approach To Construct Multicomponent HIV Vaccines. *Journal of Virology* 80: 7688–7698.
58. Maghsoodi A., Chatterjee A., Andricioaei I. & Perkins N.C. 2016. A First Model of the Dynamics of the Bacteriophage T4 Injection Machinery. *Journal of Computational and Nonlinear Dynamics* 11: 041026.
59. Žiedaitė G., Daugelavičius R., Bamford J.K.H. & Bamford D.H. 2005. The Holin Protein of Bacteriophage PRD1 Forms a Pore for Small-Molecule and Endolysin Translocation. *Journal of Bacteriology* 187: 5397–5405.
60. Kaszuba M. 2018. A basic introduction to Dynamic Light Scattering (DLS) for particle size analysis – Q&A. *Malvern Panalytical*.
61. Malvern Instruments Worldwide, Inform White Paper: Dynamic Light Scattering Common Terms Defined, Malvern Instruments Ltd., United Kingdom (2011), pp. 1–5.
62. Lim J., Yeap S.P., Che H.X. & Low S.C. 2013. Characterization of magnetic nanoparticle by dynamic light scattering. *Nanoscale Research Letters* 8: 381.
63. Malvern Instrument, Size Theory in Zetasizer Nano User Manual MAN 0485 Issue 1.1, Malvern Instruments Ltd., United Kingdom (2013), Chap. 11, pp. 1–8.
64. What is the Z-average?. Malvern Panalytical. https://www.malvernpanalytical.com/en/learn/knowledge-center/faqs/faq0015averagediameter
65. KARMAKAR, S. (no date) Particle Size Distribution and Zeta Potential Based on Dynamic Light Scattering: Techniques to Characterize Stability and Surface Charge Distribution of Charged Colloids. Available at: https://personal.utdallas.edu/~son051000/chem4473/DLSchapter.pdf (Accessed: 26 June 2024).
66. Dynamic light scattering (AKA QLS, pcs). (n.d.). https://projects.iq.harvard.edu/files/weitzlab/files/dynamiclightscattering.pdf
67. Common Terms Used In Dynamic Light Scattering. 2013. *AZO Materials*. https://www.azom.com/article.aspx?ArticleID=9924
68. Yamamoto K.R., Alberts B.M., Benzinger R., Lawhorne L. & Treiber G. 1970. Rapid bacteriophage sedimentation in the presence of polyethylene glycol and its application to large-scale virus purification. *Virology* 40: 734–744.
69. Henneberg F. & Chari A. 2021. Chromatography-Free Purification Strategies for Large Biological Macromolecular Complexes Involving Fractionated PEG Precipitation and Density Gradients. *Life* 11: 1289.
70. Dynamic light scattering Common terms defined. 2011. *www.chem.uci.edu*.
71. Tosi M.M., Ramos A.P., Esposto B.S. & Jafari S.M. 2020. Dynamic light scattering (DLS) of nanoencapsulated food ingredients. In: *Elsevier eBooks*, pp. 191–211.
72. Correction to: Rapid assessment of changes in phage bioactivity using dynamic light scattering. 2024. *PNAS Nexus* 3.

73. Mesquita M.M.F., Stimson J., Chae G. -t., Tufenkji N., Ptacek C.J., Blowes D.W. & Emelko M.B. 2010. Optimal preparation and purification of PRD1-like bacteriophages for use in environmental fate and transport studies. *Water Research* 44: 1114–1125.
74. Willey J.M., Sherwood L.M., Woolverton C.J. & Prescott L.M. 2008. *Prescott, Harley, and Klein's microbiology*. McGraw-Hill, New York.
75. Carvalho J.W.P., Carvalho F.A.O., Batista T., Santiago P.S. & Tabak M. 2014. Cetyltrimethylammonium chloride (CTAC) effect on the thermal stability of oxy-HbGp: Dynamic light scattering (DLS) and small angle X-ray scattering (SAXS) studies. *Colloids and Surfaces B: Biointerfaces* 118: 14–24.
76. Misono T. 2019. Dynamic Light Scattering (DLS). In: Abe M. (ed.), *Measurement Techniques and Practices of Colloid and Interface Phenomena*, Springer Singapore, Singapore, pp. 65–69.
77. Li, F., Hou, C.-F.D., Lokareddy, R.K., Yang, R., Forti, F., Briani, F., & Cingolani, G. (2023b). High-resolution cryo-EM structure of the Pseudomonas bacteriophage E217. *Nature Communications, 14*.
78. Butcher S.J., Manole V. & Karhu N.J. 2012. Lipid-Containing Viruses: Bacteriophage PRD1 Assembly. In: Rossmann M.G. & Rao V.B. (eds.), *Viral Molecular Machines*, Springer US, Boston, MA, pp. 365–377.
79. Archer M. & Liu J. 2009. Bacteriophage T4 Nanoparticles as Materials in Sensor Applications: Variables That Influence Their Organization and Assembly on Surfaces. *Sensors (Basel, Switzerland)* 9: 6298–6311.
80. Arakawa T. & Timasheff S.N. 1984. Mechanism of protein salting in and salting out by divalent cation salts: balance between hydration and salt binding. *Biochemistry* 23: 5912–5923.
81. Wang J., Ma J. & Wen X. 2018. Basic Concepts of Density Gradient Ultracentrifugation. In: Sun X., Luo L., Kuang Y. & Li P. (eds.), *Nanoseparation Using Density Gradient Ultracentrifugation: Mechanism, Methods and Applications*, Springer, Singapore, pp. 21–36.
82. Lark K.G. & Adams M.H. 1953. The stability of phages as a function of the ionic environment. *Cold Spring Harbor Symposia on Quantitative Biology* 18: 171–183.
83. Hatch M.T. & Warren J.C. 1969. Enhanced Recovery of Airborne T3 Coliphage and Pasteurella pestis Bacteriophage by Means of a Presampling Humidification Technique. *Applied Microbiology* 17: 685–689.
84. Ritchie D.F. 1977. Isolation of Erwinia amylovora Bacteriophage from Aerial Parts of Apple Trees. *Phytopathology* 77: 101.
85. Blazanin M., Lam W.T., Vasen E., Chan B.K. & Turner P.E. 2021. Decay and damage of therapeutic phage OMKO1 by environmental stressors. : 864025.
86. Nikulin N.A. & Zimin A.A. 2021. Influence of Non-canonical DNA Bases on the Genomic Diversity of Tevenvirinae. *Frontiers in Microbiology* 12: 632686.
87. Dynamic Light Scattering (DLS) - Definition & Terms | Malvern Panalytical. https://www.malvernpanalytical.com/en/learn/knowledge-center/whitepapers/wp111214dlstermsdefined

88. Avenue 677 Huntington, Boston & Ma 02115. 2019. Seeking the Path of Least Resistance. *Harvard Public Health Magazine*.

APPENDICES

Appendix 1: Solutions and reagents

Luria-Bertani (LB) medium	Bacto tryptone 1 % Yeast extract 0.5 % NaCl 14.5 %
Luria-Bertani (LB) agar	Luria-Bertani (LB) medium Agar 1.0%

Appendix 2: Experimental Timeline

Table A1. The timeline of experiments

Experiment	Date	Days post-Phage purification
T4		
T4 purification	24.01.2024	-
First DLS measurement	29.01.2024	5 days
First heat treatment	07.02.2024	14 days
First sonication treatment	08.02.2024	15 days
Second heat treatment	09.02.2024	16 days
PRD1		
PRD1 lysate titeration	27.02.2024	-
PRD1 purification	29.02.2024	-
First DLS measurement	01.03.2024	1 day
PRD1 heat treatment	04.03.2024	4 days
PRD sonication	05.03.2024	5 days

Appendix 3: DLS measurement of T4 Upper Pellet

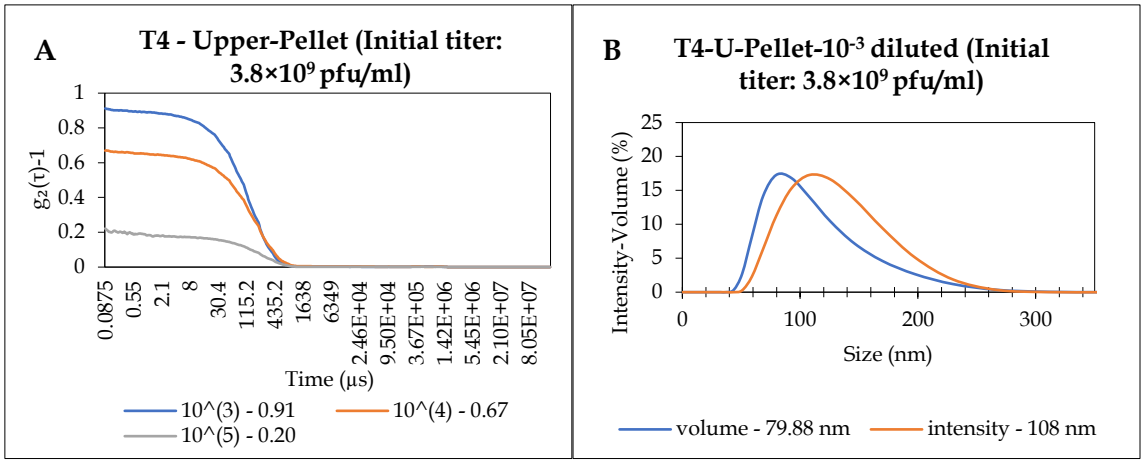

Figure 3. A) The autocorrelation function (ACF) curves were measured for T4 u-pellet with an initial titer of 3.8×10^9 PFU/mL and dilution factors of 10^3, 10^4, and 10^5. B) The intensity-weighted and volume-weighted distribution of 1000-fold diluted sample.